Energy Conversion and Management 291 (2023) 117253

Contents lists available at ScienceDirect

Energy Conversion and Management

journal homepage: www.elsevier.com/locate/enconman

Renewable and waste heat applications for heating, cooling, and power generation based on advanced configurations

Ali Khalid Shaker Al-Sayyab [a,b], Adrián Mota-Babiloni [a,*], Joaquín Navarro-Esbrí [a]

[a] ISTENER Research Group, Department of Mechanical Engineering and Construction, Universitat Jaume I, Campus de Riu Sec s/n, 12071 Castellón de la Plana, Spain
[b] Basra Engineering Technical College (BETC), Southern Technical University, Basra, Iraq

ARTICLE INFO

Keywords:
Solar-assisted heat pump
Geothermal source heat pump
organic Rankine cycle
Combined cycles
Waste heat
Trigeneration

ABSTRACT

Using renewable heat energy sources, recovering the waste heat, and enhancing the processes and energy efficiency can reduce the electricity dependency of several industrial applications. Renewable and waste heat have a low-grade enthalpic level and should be combined with other technologies to bring it to a practical level. This could be achieved by increasing the variety of heat sources and their combinations (multi-function systems), resulting in a high overall energy performance and reducing greenhouse gas emissions. Recent research on this topic has been conducted considering solar-assisted geothermal heat pumps (single and combined), low-grade waste heat, organic Rankine-vapour compression cycles (ORC-VCC), and absorption refrigeration. In the current research, comprehensively review of the state-of-the-art advanced arrangements using renewable heat sources and waste heat utilisation for simultaneous heating, cooling, and power generation was performed. To the best of the author's knowledge, the use of waste heat from VCC systems represents one of the most promising technologies in the future. Solar and geothermal heat pumps are considered for different applications and at different temperatures, presenting a high coefficient of performance. However, their utilisation is beneficial only when both renewable heat sources are considered. Although both the ORC and ejector refrigeration systems demonstrated low thermal performance, the overall system performance remained similar to that of the original system. Absorption refrigeration is promising as an up-and-coming alternative to a VCC system, but it is often hampered by excessive cooling unit sizes and a low COP.

1. Introduction

Over the past few decades, numerous environmental concerns have been caused by global warming, climate change, ozone depletion, acid rain, air pollution, waste disposal, and water pollution, all of which affect the Earth [1]. Moreover, the worldwide demand for energy and electricity is increasing rapidly [2]. Renewable resources are among the most efficient and effective solutions for developing clean and sustainable energy sources. They represent the most effective way to reduce air pollution, which is attributed to the absence of fossil fuel combustion [3].

In addition, renewable energy resources are virtually unrestricted and contribute to a reduction in electricity costs and energy dependence [4]. In the same context, with the steadily increasing environmental pollution with global energy demands growing, many worldwide agencies and institutes recommended utilising renewable energy.

The European Environment Agency analysis concluded that renewable energy reduced the use of primary domestic fossil fuels for generating energy, thereby reducing greenhouse gas (GHG) emissions in the European Union (EU) by 13% in 2018 compared with that in 2005 [3].

As Europe is 1.2 °C warmer than the average year in the 19th Century [5], the number of heat pumps in EU countries increased by 34% between 2021 and 2022, reaching approximately three million units [6]. The use of a Heating, ventilation, and air conditioning (HVAC) system provides comfort to the occupants of a building; however, in doing so, HVAC systems are likely to degrade the Earth's atmosphere. HVAC systems based on air-source heat pumps demonstrate low performance at low ambient temperatures in the heating mode and when operating at high ambient temperatures when cooling, representing a significant challenge for developing energy-efficient systems [7,8]. In 2020, the European Council endorsed the long-term goal of achieving climate neutrality by 2050 by increasing the use of renewable energy sources and improving energy efficiency [9]. Hydrofluorocarbons (HFCs) are commonly used as refrigerants in HVAC systems, and their emissions

* Corresponding author. Tel.: +34 964 728134.
E-mail addresses: ali.alsayyab@stu.edu.iq, alsayyab@uji.es (A.K.S. Al-Sayyab), mota@uji.es (A. Mota-Babiloni), navarroj@uji.es (J. Navarro-Esbrí).

https://doi.org/10.1016/j.enconman.2023.117253
Received 24 March 2023; Received in revised form 10 May 2023; Accepted 2 June 2023
Available online 24 June 2023

Nomenclature

4E	Energy, exergy, environmental, and economic
ARC	Absorption refrigeration cycle
ASHP	Air source heat pump
CO_2	Carbon dioxide
COP	Coefficient of performance
CS	Condensation system
DHN	District heating networks
DX	Direct expansion
EC	Evaporative cooling
ECACS	Evaporative cooling air conditioning system
ERC	Ejector refrigeration cycle
EU	European Union
EVCS	Ejector vapour compression cycle
FP	Flat plate collector
FTVCC	Flash tank vapour compression cycle
FTVIC	Flash tank vapour injection cycle
GHG	Greenhouse gas
GSHP	Geothermal source heat pump
GWP	Global warming potential
HFC	Hydrofluorocarbon
HP	Heat pump
HPi	Heat pipe
HVAC	Heating, ventilation, and air conditioning
IRENA	International Renewable Energy Agency
IoT	Internet of Things
IX	Indirect expansion
LCOE	Levelized cost of electricity (USD kWh^{-1})
LCPV/T	Low-concentrating solar photovoltaic/thermal
LPG	Liquefied petroleum gas
ORC	Organic Rankine cycle
ORC-CCHP	Organic Rankine cycle-combined cooling, heating, and power
ORC-CEMES	Organic Rankine cycle combined ejector multi-evaporator system
ORC-VCC	Organic Rankine cycle-vapour compression cycle
PUE	Power usage effectiveness (-)
PV	Photovoltaic
PV/T	Photovoltaic thermal
SAGSHP	Solar-assisted geothermal source heat pump
SAHP	Solar-assisted heat pump
SAHPWH	Solar-assisted heat pump water heater
SASHP	Solar-Air source heat pump
SEHP	Solar ejector heat pump system
SS	Serial system
T_e	Evaporating temperature (℃)
USD	United states dollar
VCC	Vapour compression cycle

have increased rapidly over the past two decades [10]. HFCs are potent greenhouse gases with global warming potential (GWP) values of 1430 for R134a [11] and 675 for R32 [12]. Fluorinated greenhouse gases contributed up to 2.3% of total EU greenhouse gas emissions in 2019 [13]. In 2016, the Kigali Amendment of the Montreal Protocol aimed to phase down HFCs by reducing their production and consumption to achieve over 80% to 85% reductions in HFC consumption by 2047 [14]. Nevertheless, human activities have produced a large amount of residual heat and waste heat that is contributing to climate change. Concerning global warming or climate change, it has not been seriously considered.

Several industrial processes, such as combustion, drying, heating, and cooling, dissipate waste heat into the environment. Waste heat temperature varies between industrial processes, ranging from 25 °C (for instance, in flat plate collectors) [15] up to 400 °C (ceramic production process flue gases) [16]. Accordingly, waste heat is classified as low-, medium-, or high-grade. Furthermore, waste heat recovery could be a significant source of energy efficiency for industries [17], and the food and drink processing sector contributes to 25% of the production of industrial waste heat [18].

Low-grade renewable-waste heat cannot be used directly even though can be recovered by combining it with heat pumps and upgrading to a high required level, a heat pump is a thermal system that uses electrical inputs to transfer heat from a low-temperature medium to a higher-temperature medium. Heat pump represents a promising low-carbon technology compared with the traditional fossil fuel boilers and is almost the only system available for air conditioning. When heat pumps use ambient air as a heat source, they are called air-source heat pumps, whose energy performance demonstrates fluctuations with weather conditions. Other factors can affect the freezing of the evaporator's surface in winter and high relative humidity conditions [19]. By combining it with renewable-waste heat, the overall energy performance can be increased and reduce greenhouse gas emissions by operating at high evaporation temperatures [20]. Currently, most applications are based on solar heat (solar-assisted heat pump, SAHP) [21], photovoltaic thermal waste heat (PV/T) and geothermal heat (geothermal source heat pump, GSHP) [22]. Moreover, electronic devices waste heat like the ones associated with data centre can negatively impact the environment if improperly handled.

Data centres are essential for the functioning of modern society and are designed to store, manage, and disseminate significant amounts of data. The importance of data centres in modern society cannot be overstated. They are essential for functioning businesses, governments, and other organizations that rely on technology. Mobile internet users are projected to increase from 3.8 billion in 2019 to 5 billion by 2025 [23]. The information and communications sector in the EU accounts for 2.5% of total electricity consumption (78 TWh) [24]. The Internet of Things (IoT) offers business opportunities and improves efficiency, transparency, competitiveness, and security. However, IoT often involves a large amount of data and requires new space for data centres. Global Internet traffic is expected to double by 2022 to 4.2 trillion gigabytes [23], increasing the power demand from 15% to 20% [25].

Conversely, the growth of data centres has also raised concerns about their environmental impact, contributing to approximately 2% of global CO_2 emissions, which is expected to increase in the future, according to the Environmental Protection Agency (EPA) [26]. They consume vast amounts of energy and produce significant amounts of heat removed by the cooling system to protect the electronic components from damage, resulting in an electricity consumption representing 40% of the total consumption [27]. Reducing the operating costs (caused by the electricity consumption of data centres and cooling systems) and the associated carbon footprint are two of the biggest challenges faced by data centres. To address these issues, research on data centre cooling and waste-heat injection into district heating networks (DHNs) is becoming increasingly crucial for cooling and heating applications.

Another promising technology for low- and medium-grade renewable-waste heat utilisation is the organic Rankine cycle (ORC), which uses different heat sources for electricity generation [28]. However, this technology demonstrates low energy efficiency compared with other power cycles owing to low temperature lift (temperature difference between the heat sink and the source) [29]. The VCC can be combined with ORC to increase the energy efficiency of the ORC [30].

The energy performance of the heat pump is a key factor in the industrial, commercial, and building sectors. Different arrangments combining heat pump technology with waste and renewable heat have

been intensively studied in recent years. Moreover, this enables the transition from a single-purpose vapour-compression system to a simultaneous heating and cooling system. When combined with thermodynamic systems operating at a feasible temperature range, these systems can produce renewable electricity, resulting in trigeneration or combined heating, cooling and power systems. This study presents a literature review of the methods used to increase energy performance and reduce the carbon footprint of heat pumps through effective and technically viable renewable heat energy and waste heat utilisation. The current study focuses on PV/T and data-centre waste heat because they are commonly combined with heat pumps. The remainder of this study is organised according to heat input: the assessment of heat pumps with solar and PV/T waste-heat inputs is described in Section 2; heat pumps combined with geothermal heat sources are reviewed in Section 3; an overview of heat pumps using solar and geothermal sources is presented in Section 4; various techniques for data centre waste-heat utilisation is discussed in Section 5; and the combined ORC and refrigeration systems based on solar and geothermal heat are reviewed in Section 6. These five sections include the analysis of the techniques used for improving the overall energy performance of advanced heat pumps through combination with other technologies. Finally, in Section 7, the main conclusions of this study are summarised.

2. Solar energy

2.1. Background

Solar energy is clean, readily available, renewable, and can be converted into thermal or electrical energy. Solar thermal technologies usually produce moderate-temperature heat that cannot be applied to industrial heating. These systems can be used as heat sources for heat pumps when coupled with flat-plate collectors or PV/T panels, Fig. 1 shows the SAHP coupling possibility. SAHPs can increase the ability of a solar collector to absorb solar radiation, increase the overall energy efficiency, or generate electricity by reducing the PV/T panel's operating temperature. In addition, the SAHP operates at higher evaporation temperatures than conventional fan coil systems, absorbing less electric power [31].

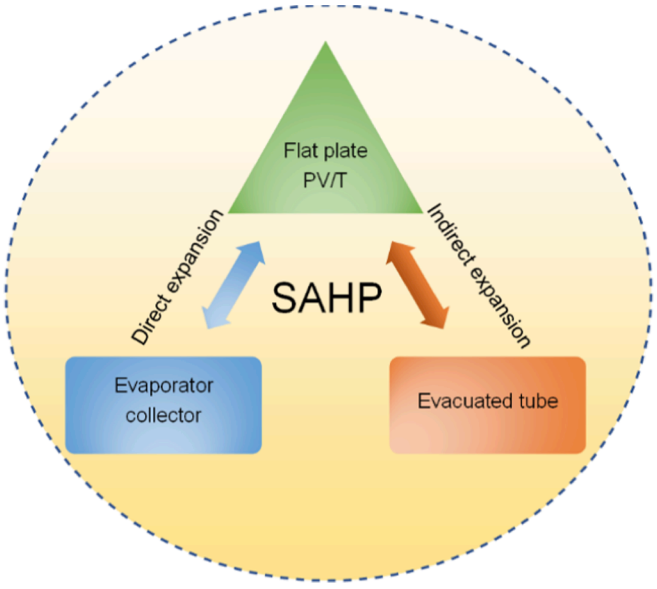

Fig. 1. Solar-assisted heat pump possibilities.

There are two methods for combining heat pumps and solar energy technologies, as shown in Fig. 1. The first method is a direct-expansion SAHP (DX-SAHP); another possibility is an indirect-expansion SAHP (IX-SAHP). From Fig. 2, comparing the two arrangements, in the case of DX-SAHP (Fig. 2.a), the flat plate or a PV/T panel acts as the heat pump evaporator and the refrigerant flows directly into the coil (refrigerant in direct contact with the solar energy no secondary circuit) [32], the collector was more efficient operating at low temperature compared to IX-SAHP, so has no additional heat exchanger or pump for the secondary circuit it's required less operating power. It's a more efficient, environmentally friendly, and cost-effective way compared to IX-SAHP. Still, it requires more refrigerant with a long connection pipe, which can increase the risk of leaks, environmental risks when using high GWP refrigerants, and other maintenance issues. While another possibility is an indirect-expansion SAHP (IX-SAHP), as shown in Fig. 2.b, the secondary fluid circulates between the solar collector or the PV/T panel. It requires an additional heat exchanger as a secondary circuit water pump. In this case, the collector operates at a moderate temperature (compared with DX-SAHP). Compared to DX-SAHP, this option was less efficient, requires more heat exchangers, consumes more electricity (secondary circuit water pumps), is more expensive and causes a more significant pressure drop, but less refrigerant charge with less refrigerant leakage possibility.

2.2. Technologies applied for combining the heat pump and solar energy

2.2.1. Flat plate collector

The solar collector works as a heat pump evaporator (in the case of DX-SAHP), wherein the refrigerant absorbs the heat collected through solar thermal conversion and from the ambient air. The refrigerant temperature is significantly lower with a low collector surface temperature, which can consequently utilise solar radiation more efficiently than conventional solar water heating systems. In the case of IX-SAHP, the solar collector acts as a heat source, although this arrangement has a lower efficiency and requires a higher number of heat exchangers and pumps but less refrigerant charge.

With the increased awareness of energy and heat pump performance enhancing, many authors have conducted simulations to evaluate the performance of direct expansion solar-assisted heat pumps. Sun et al. [34] optimised a channel roll-bond collector/evaporator using T-shaped and honeycomb-shaped patterns. They proved that the new optimised patterns enhanced the performance of the system. The T-shaped channel pattern showed the highest COP enhancement of 14.6% and a heating capacity of 17.3% compared with the conventional parallel channel pattern. Chow et al. [32] demonstrated that a DX-SAHP performed better than a conventional heat pump, with a yearly average COP of 6.5. Kong et al. [35] simulated an R410A DX-SAHP and showed that the meteorological parameters significantly influenced the thermal performance of the system. Increasing the ambient temperature from 0 °C to 35 °C lowers the heating time by 28.4% and increases the average COP by 56.4%. Fernández-Seara et al. [36] tested a DX-SAHP for water heating under zero solar conditions with a 300-litre storage tank and found the system's COP to be 3.2. Kong et al. [37] simulated a DX-SAHP using a flat-plate bar collector as an evaporator. They showed that an increase in the compressor speed slightly influenced the COP. However, the ambient temperature and solar radiation increased the system's COP. Furthermore, wind speed has a negligible effect on the system's performance.

2.2.2. Photovoltaic cells-solar waste heat

Photovoltaic cells (PV) cells convert solar energy into electrons in silicon semiconductors to generate electrical power. During this process, heat is generated in the cells; however, not all solar energy is converted into electricity, resulting in energy loss (waste heat). The heat generated in the PV cell is poorly transferred from the PV module to ambient air. Owing to the increased cell temperature, the number of electrons in

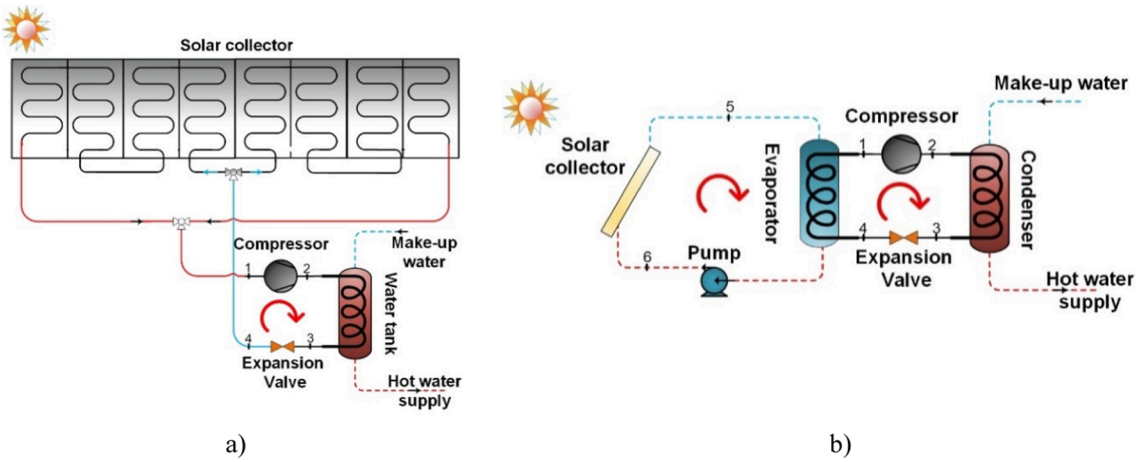

Fig. 2. Solar-assisted heat pump (a) direct expansion, and (b) indirect expansion. Adapted from Li et al. [33] and Chow et al. [32], respectively.

silicon semiconductors decreases, and the power output is reduced. However, the interest in PV technology is related to improving the overall performance of the PV system. Several studies have proposed PV/T-based technologies to reduce the PV operating temperature, increase the electric efficiency, and utilise waste heat as a heat pump evaporator or heat source for other purposes [38]. PV/T systems can simultaneously supply solar and thermal energies, wherein PV/T collectors use solar radiation more efficiently than PV modules or solar thermal collectors alone.

The performance of PV/T systems is highly dependent on the availability of sunlight. However, on overcast days, the amount of sunlight reaching the PV panels is significantly reduced, affecting their performance, so as a heat pump. On overcast days, the thermal component of the PV/T system can still generate heat energy from the ambient temperature, but still insufficient. The PV/T-heat pump system combined with other thermal technologies can improve energy efficiency and reduce heat pump consumption power. Heat pumps can be connected to an additional air-source heat exchanger and a PV/T. This increases the ability of the system to respond to domestic hot water/heating loads at low solar radiation, as proved experimentally in a previous study [39]. Other authors have modified the design of the heat exchanger using a mini-channel heat exchanger for air sources and PV/T. The heat transfer coefficient and PV/T thermal and electrical efficiencies increased in a multi-function PV/T-SAHP for hot water, heating, and power generation [40]. The multi-functional PV/T-SAHP (heating, providing domestic hot water, cooling, and power generation) outperforms the energy performance of the standard ASHP [41]. A few studies have included heat pipe technology in PV/T panels and an air source heat exchanger to increase the thermal and electrical efficiency in hot water production as shown in Fig. 3 [42–44]. In this arrangement shown in Fig. 3, there are two independent flow channels; the evaporated fluid would be delivered through the vapour line (by buoyancy force) into the flat-plate heat exchanger. At the same time, the condensed liquid can return through the liquid line (by gravity) into the heat pipe evaporator, where the evaporation process takes place by absorbing PV/T waste heat.

In line with the 2020 Vision for Europe, several studies have focused on integrating ejectors into heat pumps to maximise the system's overall performance. The ejector is a device with no moving parts and consists of two nozzles (converging and diverging) that convert dynamic pressure into static pressure or vice versa. It can be used as an expansion device for heat pumps [45] or to increase condensing pressure [46]. In the same context, heat generated from a flat plate or a PV/T panel has been used as an ejector driving force to increase the vapour compression efficiency of the heat pump for heating, providing hot water, cooling, and power generation refer to Fig. 4.

From Fig. 4.a, the system, in this case, uses PV/T waste heat as a driving force for an ejector while exploiting the generated electric power to operate the heat pump compressor and pumps. Including an ejector in solar-assisted heat pump configurations could benefit the system performance by reducing the compressor power consumption by reducing the compressor pressure ratio. Whereas in Fig. 4.b, the system uses waste heat from the PV/T panel as a heat source for the generator and maximizes the PV/T power by decreasing the operating temperature, the system includes an ejector, an ejector pump, generator, and waste heat recovery heat exchangers. The waste heat exchanger uses the condenser waste heat to enhance the system performance and allows the system to operate with enhanced COP at zero solar intensity (overcast day conditions).

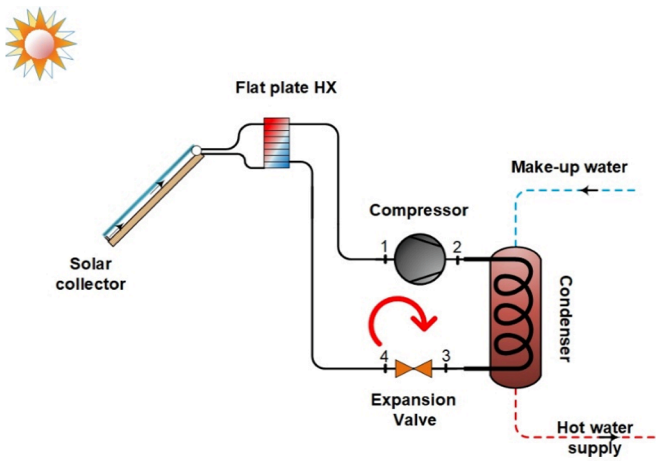

Fig. 3. Solar assisted/heat pipe-compound heat pump. Adapted from Zhang et al. [43].

Several studies have proposed different ejector–heat pump arrangements according to the final purpose. The waste-heat–driven ejector in the solar collector increased the heating capacity and COP of DX-SAHP [47]. For cooling purposes, Xu et al. [48] developed a system that reduced the costs by 24% compared with a conventional chiller. Al-Sayyab et al. [20] presented a modified PV/T waste heat ejector-compound heat pump with low global warming potential refrigerants for cooling and heating applications; in the cooling mode, the application of heat exchanger waste heat recovery enhances the system COP from 3.7 to 4 at overcast day conditions and evening conditions.

2.2.3. *Energy exergy performance comparison*

The comparison between SAHP and ASHP from an Energy-Exergy

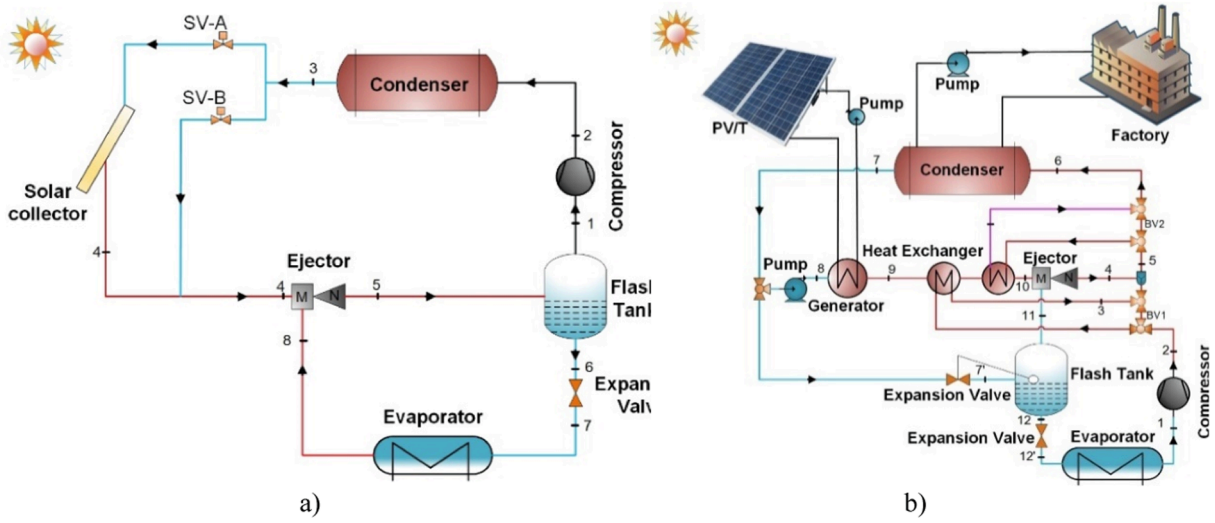

Fig. 4. Solar-assisted compound ejector heat pump: (a) direct expansion, adapted from Chen and Yu [47] and (b) indirect expansion, adapted from Al-Sayyab et al. [20].

vision is an exciting topic widely discussed in many studies. It is clear that the SAHP offers significant energy efficiency and sustainability advantages. The main difference between these two systems lies in their approach to energy efficiency. Overall, DX-SAHP and IX-SAHP are effective heating and cooling solutions compared to ASHP.

2.2.3.1. Energy analysis. An essential parameter for measuring the heat-pump performance is the COP, which is the ratio of the condenser heating capacity to the compressor power consumption. Conventional heat pumps (air source heat pumps [ASHP]) consume large amounts of power under cold weather conditions (low evaporation temperatures and pressures result in a high-pressure ratio). Fig. 5 shows that when a heat pump is combined with a solar heat source, the power consumption of the heat pump decreases compared with that of the ASHP. The highest reduction is observed during periods of high solar intensity.

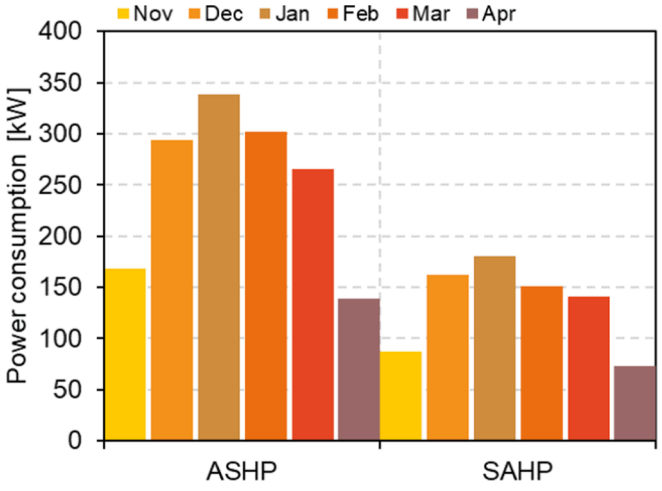

Fig. 5. Power consumption in winter for SAHP and ASHP. Adapted from Tzivanidis et al. [49].

As shown in Fig. 6, the COP of SAHP increased by 28% on average compared with that of ASHP [50]. Despite this benefit, the energy performance of SAHP can be reduced during an overcast day or in the absence of solar energy compared with ASHP, as explained in Fig. 7; also, as the supply water temperature increases, the system performance is reduced gradually owing to an increase in consumption power for given source conditioning. Additional heat sources, such as geothermal sources, provide support to the system to achieve stable performance on overcast days or at midnight.

2.2.3.2. Exergy analysis. Fig. 8 shows that increasing the solar intensity decreases the overall exergy efficiency of SAHP owing to the exergy destruction of the collector, despite reducing it for other components [47]. In fact, solar energy increases the overall efficiency of the system except for the solar collector, which has been proven in a few studies [47]. The ejector comprises the most significant exergy destruction percentage if the solar collector's contribution to the second law analysis is neglected, as demonstrated by Li et al. [53], and Al- Sayyab et al. [54].

Table 1 summarises the studies on heat pumps combined with solar renewable heat. From the analysis of the data given in this table, it can be concluded that most studies have focused on combined PV/T heat pump technologies because PV/T panels provide electrical and thermal energy. In addition to the initial cost, it has a significantly lower operational cost than other alternatives. This increases the overall performance by reducing the PV/T operating temperature and power consumption of the heat pump (higher evaporating temperature). Furthermore, this system reduces electricity consumption and greenhouse gas emissions, benefiting the economy and environment.

The flat-plate and PV/T-based heat pump combination is suitable for heating and providing domestic hot water without accounting for cooling. Most studies have relied on R134a and R22 as refrigerants because they are widely used in refrigeration systems; only a few have focused on refrigerants with a low GWP. The combined solar-driven ejector-heat pump (SEHP) system has been adopted by researchers in several studies for cooling purposes only, thus increasing the system's overall performance compared with conventional heat pumps and SAHP (because of reduced power consumption by the compressor).

The use of multi-function solar-driven ejector heat pumps for

simultaneous cooling, heating, and power generation appears to be promising. Increasing the energy performance of these systems is essential for widespread their use. One approach is to extend the variety of heat sources, such as geothermal or data centres, modify the PV/T coil design, or combine them with heat pipes.

2.3. Solar coupling summary

In light of section 2, heat pump solar coupling is generally unstable owing to seasonal and weather fluctuations. So as all types of solar coupling require an additional storage tank or phase change material to extended operational periods with stable performance, but this is still

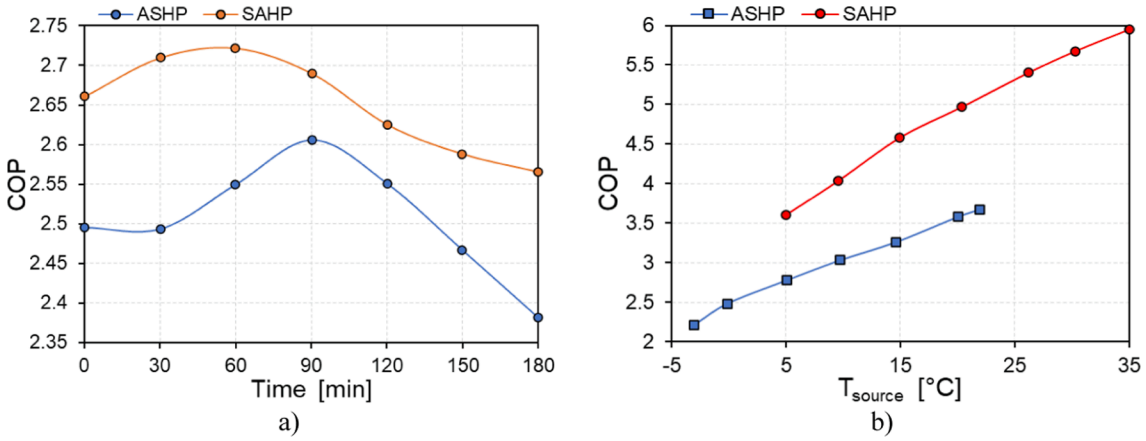

Fig. 6. Comparison of the COP values of SAHP and ASHP: (a) over a different period and (b) different source temperatures. Adapted from Jie et al. [50] and Bellos et al. [51], respectively.

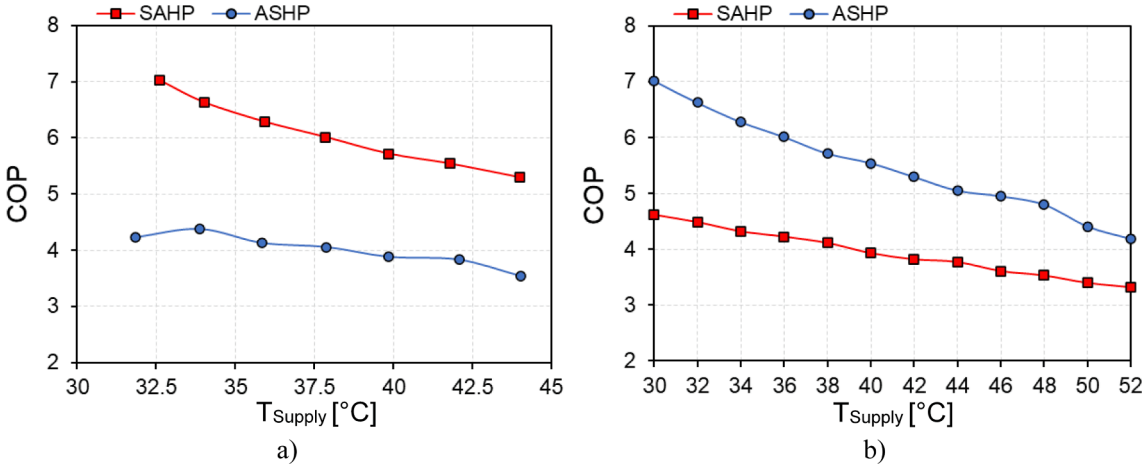

Fig. 7. Comparison of the COP values of SAHP and ASHP over different heat source temperatures: (a) highest solar intensity and (b) at night. Adapted from Sun et al. [52].

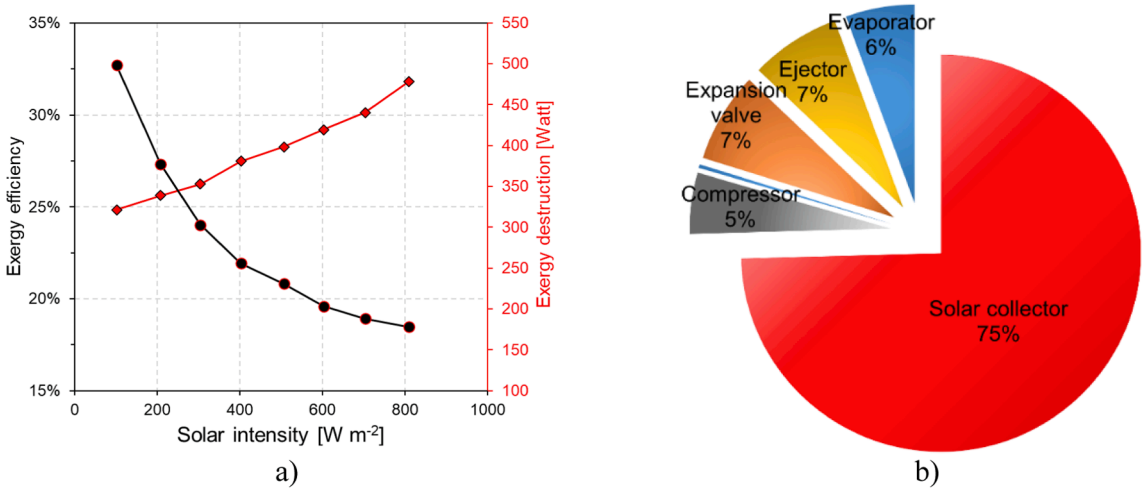

Fig. 8. Exergy performance: (a) over solar intensity, and (b) percentage exergy destruction. Adapted from Chen et al. [47].

Table 1
Overview of SAHP studies (continued).

Reference	Configuration	Purpose	Refrigerant	Heat source	Type of analysis	Concluding remark
Sun et al. [34]	DX-SAHP	Heating	R134a	Flat plate collector	Energy/Experimental	Experimentally proved that the new optimised T-shaped channel pattern enhances the system performance and showed that the system's COP is enhanced by 14.6% and the heating capacity by 17.3% compared with the conventional parallel channel pattern.
Kong et al. [37]	DX-SAHP	Heating	R22	Flat plate collector	Energy/Simulation	The increase in the compressor speed reduces the system's COP; however, an increase in the ambient temperature and solar radiation influences the system's COP. By contrast, wind speed has a non-significant effect on the system's performance.
Chow et al. [32]	DX-SAHP	Heating	R134a	Solar collector	Energy/Simulation	The results show that the DX-SAHP performs better than the conventional heat pump, with an average yearly COP of 6.46.
Kong et al. [35]	DX-SAHP	Heating	R410A	Solar collector	Energy/Simulation	An increase in the ambient temperature reduces the heating time by 28.4%, with the average COP increasing by 56.4%.
Fernández-Seara et al. [36]	DX-SAHP	Heating	R134a	Solar collector	Energy/Experimental	Using a storage tank benefits system's COP with a maximum value of 3.23 under zero solar radiation conditions.
Xu et al. [55]	DX-SASHP and water heater	Domestic water heating	R22	Solar collector	Energy/Simulation	The operation was not constrained by adverse weather conditions and could produce hot water on a round-the-clock basis, with improved overall energy efficiency.
Xu et al. [56]	IX-SEHP	Cooling	R290, R134a, R1234ze(E), R152a, and R600a	Flat plate collector	Energy and exergy/ Simulation	The R152a system results in the highest COP and high electric efficiency. The system's COP increases the conventional ejection–compression cycles by up to 22.8%.
Arbel and Sokolov [57]	IX-SEHP	Cooling	R142b and R114	Flat plate collector	Energy/Simulation	The cost–benefit ratio is reduced by reducing the collector's size. The R142b system shows a higher performance than the R114 system.
Xu et al. [48]	IX-SEHP	Cooling	R152a	Flat plate collector	Exergy and economic/ Simulation	There is a higher exergy and energy performance than a conventional system, with a total cost reduction of 24.4%.
Xu et al. [58]	IX-SEHP	Cooling	N/A	Flat plate collector	Energy/Simulation	The system shows an electric reduction of 11.8% than the cooling system based on the conventional ejection-compression refrigeration cycle.
Wang et al. [59]	IX-SEHP	Cooling	R245fa, R1233zd(E) and R1336mzz(Z)	Solar collector	Energy/Simulation	R1233zd(E) and R1336mzz(Z) reduce compressor power consumption to 14.6% and 38.1% compared with R245fa. The system COP in heating mode is 3.75.
Chesi et al. [60]	IX-SEHP	Cooling	R134a	Solar collector	Energy/Simulation	The average yearly COP is increased by 15% compared to a conventional system.
Sun [61]	Dual fluid DX-SEHP	Cooling	Steam-R134a	Solar collector	Energy/Simulation	The system saves more than 50% on energy consumption, with a 50% reduction in greenhouse gas emissions, compared to a traditional heat pump.
Li et al. [53]	Dual fluid DX-SEHP	Cooling	VCC: R1234yf and R134a ERC: R141b and R1234yf	Solar collector	Energy and exergy/ Simulation	R1234yf-R141b system shows a high energy and exergy performance compared to a conventional heat pump.
Dang [62]	Dual fluid IX-SEHP	Heating and cooling	R1234ze(E) and R410A	Solar collector	Energy/Simulation	The system achieves energy saving in the heating and cooling modes up to 50% and 20%, respectively, compared with a traditional heat pump.
Chen and Yu [47]	DX-SEHP	Hot water	R134a	Solar collector	Energy and exergy/ Simulation	The increase in solar intensity has a beneficial effect on the energy performance of the cycle but has a decreased effect on exergy efficiency. The system's COP increased by 13.8%, and the heating capacity increased by up to 20.4%.
Ji et al. [63]	PV/T-DX-SAHP	Heating and power	R22	PV/T and flat plate	Energy/Experimental	This system increased the PV/T efficiency by 13.4% and presented a higher COP than that of a conventional heat pump with an average COP of 5.4.
Kuang and Wang [64]	DX-SAHP	Heating, air conditioning, and domestic water heating	R22	PV/T	Energy/Experimental	The system produced 200–1000 L of hot water at 50 °C with a COP ranging from 2.1 to 2.7 and relatively low running costs under various weather conditions in Shanghai. The thermal storage tank is beneficial as it reduces the compressor's operating period in the space-cooling mode.
Li et al. [21]	PV/T-DX-SAHP	Heating and power	R22	PV/T	Energy and exergy/ Experimental	The compressor and collector/evaporator represent the largest sources of exergy destruction, while the expansion valve represents

(*continued on next page*)

Table 1 (*continued*)

Reference	Configuration	Purpose	Refrigerant	Heat source	Type of analysis	Concluding remark
						the smallest. The system with a small collector/evaporator area has a lower capital cost and can be easily integrated into the building's roof.
Ji et al. [65]	PV/T-DX-SAHP	Heating and power	R22	PV/T	Energy/Experimental and simulation	The developed combination system shows an increase in the overall performance, with a maximum COP of 8.4 and an average value of 6.5, whereas the average PV/T efficiency was approximately 13.4%.
Xu et al. [66]	PV/T-DX-SAHP	Heating and power	R22	PV/T	Energy/Simulation	The system demonstrates an efficient simultaneous heating and power production. The system's COP and thermal efficiency increased by 7% and 6%, respectively, compared with conventional PV/T-HP systems.
Fang et al. [67]	PV/T-DX-SAHP	Heating and power	R134a	PV/T	Energy/Experimental	It performs above a conventional heat pump, and the PV/T efficiency improved by 23.8% compared to the conventional module, with 2.88 heat pump mean COP.
Mastrullo and Renno [68]	PV/T-DX-SAHP	Heating and power	R22	PV/T	Energy, exergy and economic/Simulation	A higher COP than a traditional system. Solar intensity increases energy and exergy performance.
Zhao et al. [69]	PV/T-DX-SAHP	Heating and power	R134a	PV/T	Energy/Experimental	The proposed combination system shows significant savings in capital and running costs over separate arrangements of PV, heat pump, and roof structure, with thermal, electrical and overall efficiencies of 55%, 19%, and 70%, respectively.
Keliang et al. [70]	PV/T-DX-SAHP	Heating and power	NA	PV/T	Energy/Simulation	The average COP of the system reached 6.0, and the average electrical, thermal, and overall efficiencies were 14%, 48% and 63%, respectively.
Chen et al. [71]	PV/T-DX-SAHP	Heating and power	R134a	PV/T	Energy/Experimental	Solar radiation benefits the system's COP. The condenser's supply temperature and flow rate decreased the COP. The electrical efficiency of the PV/T panel was improved by 1.9%.
Wang et al. [72]	PV/T-IX-SAHP	Heating, cooling, and power	R407C	PV/T	Energy/Experimental and simulation	The system enables hot water production with less electric consumption and a higher COP than a solar water heater and a domestic heat pump on cloudy days and winter conditions.
Ji et al. [73]	FP-PV/T-DX-SAHP	Heating and power	R22	PV/T and flat plate	Energy/Experimental and simulation	The system demonstrates high performance, with the PV/T's electrical and thermal efficiencies of above 12% and 50%, respectively.
Chaturvedi et al. [74]	Two-stage DX-SAHP	Heating	R134a	Solar collector	Energy/Simulation	The two-stage SAHP notably increased the thermal performance and has higher performance and capital cost than a single-stage SAHP.
Cai et al. [75]	PV/T-IX-SAHP	Heating, cooling, and power	R134a	PV/T	Energy/Experimental and simulation	The system met the requirement for space heating, cooling, and water heating with COP of 2.57 at 800 W/m^2 of solar irradiation.
Fu et al. [42]	VCC-HPi-PV/T	Heating and power	R134a	PV/T	Energy and exergy/ Experimental	The daily average energy efficiency of the system was 61.1–82.1%, and exergy efficiency was 8.3%–9.1%, with an average COP of 4 of the heat pump.
Zhang et al. [43]	VCC-HPi-PV/T	Power and hot water	R134a	PV/T	Energy and exergy/ Experimental	Thermal, overall, energetic, and exergetic efficiencies of the system were 9.1%, 39.3%, 48.4% and 15.0%, respectively, with a COP of 8.7.
Zhang et al. [44]	VCC-HPi-PV/T	Heating and power	R134a	PV/T	Energy/Experimental and simulation	The heat pipe increased the overall performance. The overall COP was 8.7, and the electrical and thermal efficiencies were 10% and 40%, respectively.
Wang et al. [76]	IX-SASHP	Heating and power	N/A	PV/T and water solidification process	Energy/Experimental and simulation	The system demonstrated operational stability and reduced the peak power grid load, with an average COP of 2.6.
Al-Sayyab et al. [20]	Compound waste heat-solar driven ejector-SAHP	Simultaneous heating and cooling	R134a, R450A, and R513A	PV/T and condenser waste heat	Energy/Simulation	R450A shows system COP improving by 7% and 5% in cooling and heating mode compared to a conventional R134a system. Waste heat recovery increases the system COP from 3.7 to 4 without solar radiation.
Al-Sayyab et al. [77]	Compound PV/T waste heat driven ejector-HP	Simultaneous heating – cooling, and power	R134a	PV/T waste heat	Advanced exergoeconomic/ Simulation	The compressor represents the largest exergy destruction source (26%), while the generator is the lowest. 59.4% of the exergy destruction can be avoided when the system is optimised.

(*continued on next page*)

Table 1 (*continued*)

Reference	Configuration	Purpose	Refrigerant	Heat source	Type of analysis	Concluding remark
Al-Sayyab et al. [54]	Compound PV/T waste heat-driven ejector-HP	Simultaneous heating and cooling	R450A, R513A, R515A, R515B, R516A, R152a, R444A, R1234ze(E), R1234yf, R290, and R1243zf	PV/T waste heat	Energy, exergy and environmental/ Simulation	Compared to a traditional R134a heat pump, the system with R515B presents the highest COP increase, 54% in cooling and 49% in heating.
Lu et al. [78]	Absorption	Heating and cooling	LiBr	Solar and biomass	Energy/Simulation	The operational cost of 25.5% to 46.8% of the system is lower than that of a traditional gas furnace/compression heat pump, and CO_2 emissions are reduced by 16% and 20%.
Xu et al. [79]	DX-SEHP	Cooling	R600a	Low-grade waste heat	Energy/Simulation	The system demonstrated a 24% higher COP than a conventional system but slightly lower than an ejection vapour compression cycle.

inefficient for prolonged periods in contrast to the weather conditions or fluctuations. DX-SAHP coupling presents a compact system with efficient energy and economic performance compared with ASHP and IX-SAHP owing to the flat plate-PV/T operating at low temperatures with fewer components (heat exchangers and pumps). This type still requires a more refrigerant charge, a supplementary electric power source (in case of flat plate), proper component configuration to prevent refrigerant leakages, and heat loss reported (in case of flat plate), more difficult for installation compared with IX-SAHP. In IX-SAHP coupling present system has more flexibility and is easy to install. It requires a less refrigerant charge, so there is a less direct global warming effect, but more complexity and several components (heat exchangers and pumps) with less energy performance and high cost. PV/T coupling is a promising technology that presents an efficient system with green electric energy that can be used for heat pump operations. Using heat pipe in PV/T-IX-SAHP saves energy with less cost (eliminating the water pump).

3. Geothermal

3.1. Background

Geothermal energy is decarbonised, non-polluting, reliable, sustainable, and potentially environmentally friendly (the emissions of geothermal electric power plants are 97% lower than those of fossil fuel power plants of similar size as well as 99% lower than carbon dioxide emissions) [80,81]. In addition to being used for heating and cooling, it can generate clean electricity. It is independent of weather conditions, not intermittent, and can be easily integrated into the buildings. Contrary to the wind and solar power, the energy source has a capacity factor of up to 96% (Fig. 9) [82]. Geothermal heat sources connected to heat pumps offer an almost constant temperature, thereby reducing the primary energy consumption and CO_2 emissions. By 2050, geothermal power generation is expected to increase to up to 800% compared with that in 2020 [83].

Traditional heating systems can be replaced with geothermal-source heat pumps. Geothermal-source heat pumps (GSHP) have several advantages over ASHPs, they are more energy-efficient than traditional heating systems because they can use the more stable temperature of the earth as the evaporator heat source. Despite the fact that both geothermal and traditional systems require electricity to operate, geothermal systems use less energy overall, so it's more efficient than ASHP (lower power consumption by the compressor), have a simple design, and require less refrigerant charge and maintenance [85].

Many studies adopted many arrangements to increase system stability [86,87]. Fig. 10 shows an example of a different GSHP arrangement in Fig. 10.b the modified arrangement implements a storage tank to increase system stability with a multistage of heat exchange; this arrangement consumed more power compared with GSHP owing to the number of circulating pumps but presented more system stability.

GSHP has recently received more attention owing to its advantages. In Europe, countries with cold climates are experiencing an increase in the use of GSHP. Colder countries, such as Sweden, use the highest proportion of GSHP units among European countries, followed by Germany (Fig. 11). By contrast, ASHP is the most widely used in Italy [86].

A few studies have evaluated the potential of GSHP in terms of energy efficiency increase. Maddah et al. [86] proved that a GSHP demonstrates higher energy performance than an ASHP. Another study revealed that GSHP and compound-wall GSHP exhibited higher energy performance and required less fuel consumption than other heating systems. Hepbasli et al. [85] recommended the prevention of component oversizing to improve the system's performance. Akbulut et al. [87] proved that a vertical-wall GSHP demonstrates the highest efficiency, COP, and lowest fuel consumption for heating, considering several heating systems.

Like the previous section, Table 2 is presented. Most studies have concluded that GSHP increases the overall performance compared with

a conventional ASHP, with economic and environmental benefits, by reducing power consumption and greenhouse gas emissions. Most studies used R134a as a working refrigerant and focused on the thermal performance without accounting for the global warming effect or increasing the performance with the use of low-GWP refrigerants.

3.2. Geothermal coupling summary

heat pump geothermal coupling is generally more stable than SAHP. Still, over an extended operational period, GSHP demonstrates performance fluctuations in cold climates (low heating capacity and uncomfortable indoor air temperatures). This is because the heat extracted from the soil in the heating mode is higher than that injection into the soil in the cooling mode [93]. An auxiliary heat source can stabilise the performance of GSHP for an extended period for heating purposes. Non-renewable auxiliary heat source coupling has a detrimental environmental effect as it increases greenhouse gas emissions. Various types of renewable heat sources can be used to overcome the thermal imbalance encountered in conventional geothermal-source heat pump systems. In addition, using a storage tank with a phase change material can increase the system's stability. But may not be enough benefits to offset the costs when shallow geothermal resources are available. Finlay, Because of their interaction with geothermal fluid, GSHP systems suffered performance degradation for long periods of operation due to corrosion and scaling in the underground heat exchangers. Therefore, it was necessary to clean, replace, and, in troubled cases, perform extensive repairs with this type of coupling.

4. Solar and geothermal

4.1. Background

Despite their high efficiency, SAHPs are unstable owing to seasonal and weather fluctuations. The GSHP demonstrates COP fluctuations after an extended operational period (such as a decrease in the ground temperature; therefore, the heat pump is operated at a higher-pressure ratio). In cold weather, there is a reduction in the soil temperature, which may lead to disturbances in the soil temperature balance and deterioration in the performance of the GSHP performance [94]. The GSHP was combined with a solar heat source to achieve a stable heat supply, resulting in solar-assisted geothermal-source heat pumps (SAGSHPs). Supporting the SAGSHPs with supplementary heat sources and heat storage devices is recommended [95]. Studies have suggested that solar-assisted heat pump efficiency can be enhanced by geothermal heat sources. Yang et al. [96] proved that SAGSHP reduced electricity consumption by 10.4% and 14.5%, and Xi et al. [97] showed that a SAGSHP increases heating efficiency by 26.3% compared with a standard GSHP. Wang et al. [98] experimentally confirmed that SAGSHP

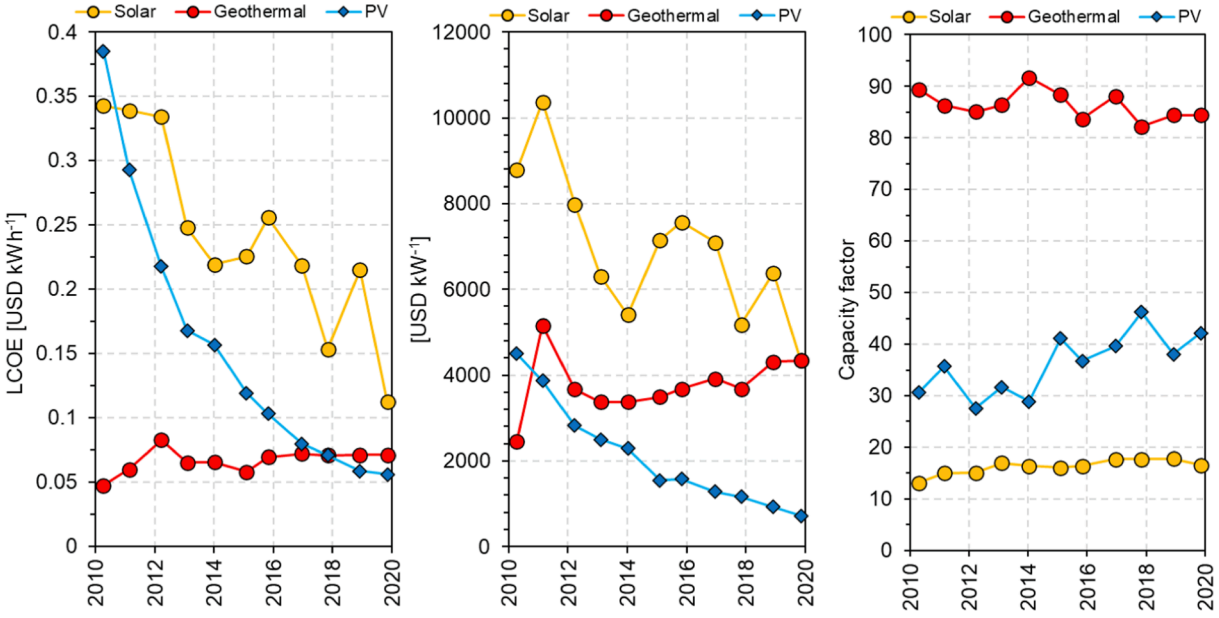

Fig. 9. Renewable energy technologies cost and performance. Adapted from IRENA [84].

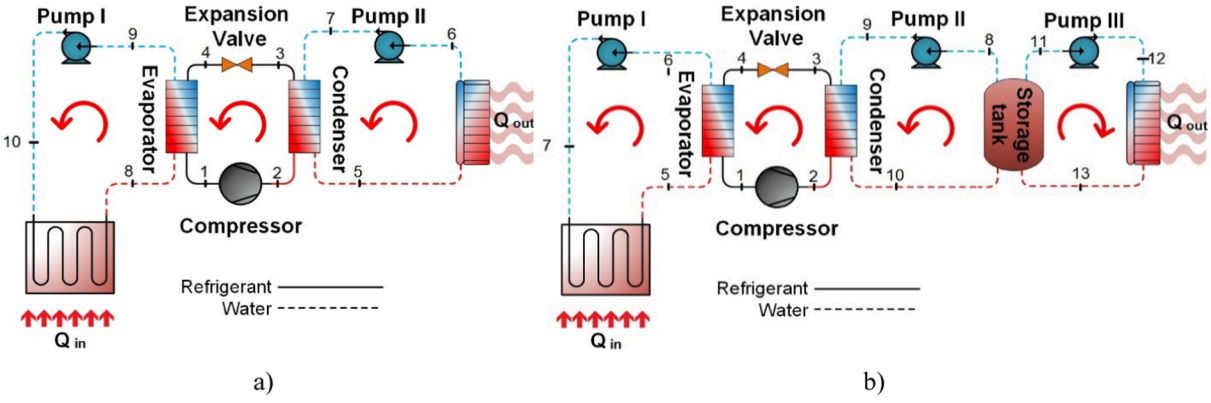

Fig. 10. Geothermal source heat pumps. Adapted from: (a) Maddah et al. [86], and (b) Akbulut et al. [87].

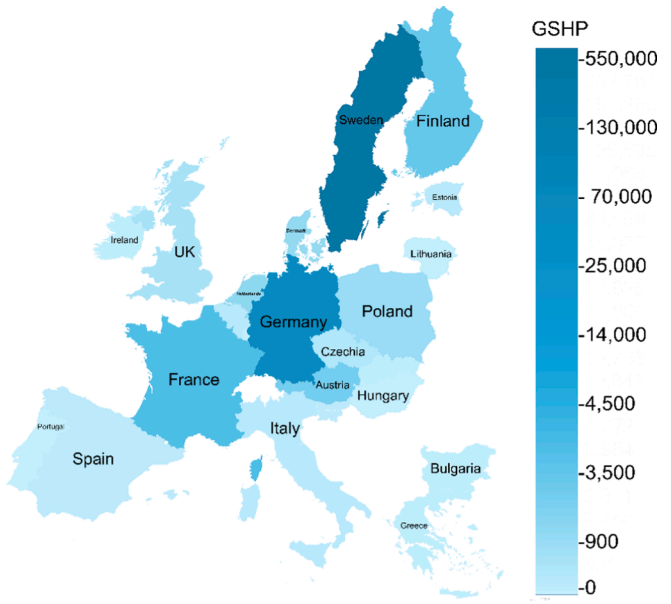

Fig. 11. Number of GSHP in European countries [88].

reduces electricity consumption and increases the COP.

Fig. 12 shows two different SAGSHP arrangements; in the case of Fig. 12.a the solar collectors are primarily used for domestic heat water heating, injected into the ground once the temperature is reached; this prevents collector overheating and contributes to ground load balance. In addition to heating, the heat pump can also be cooling. In the case of Fig. 12.b typically, heat sources come from solar and heat pumps. Heat storage tanks are controlled to maintain a specific temperature for heating and hot water supply. As the collector acquires the heat, it is transferred to a thermal heat storage tank. A heat pump operates when the temperature in a storage tank is below the designed temperature, supplying insufficient heat. The system implemented two different temperature heat exchanger levels in order to control the supply temperature.

Fig. 13 shows that SAGSHP demonstrated an increase in performance from 17% to 22% [100], and the highest increase (30%) was recorded at mid-day [96] when the solar intensity reached the maximum value. Contrarily, the lowest increase in energy performance of 6% was reported at sunset.

From the studies summarised in Table 3, All these studies focused on flat-plate solar collectors and did not include renewable electricity sources for water circulation pumps. Future studies focussing on PV/T panels are highly recommended. Most studies have used R22 as the working fluid because of its promising thermal performance without accounting for its effect on the climate and ozone layer. Therefore, studies should consider low-GWP refrigerants to increase environmental benefits by reducing power consumption and greenhouse gas emissions.

4.2. Solar-Geothermal coupling summary

It can be concluded that the solar-geothermal heat source heat pump stabilises the heating performance under different operations (overcast or sunrise, sunset, and night), in addition to increasing the overall heating performance. This system is more complex, with more heat exchangers and pumps than the current alternatives. The complexity of integrating two different systems should be carefully designed to increase the overall performance and prevent component oversizing, which can degrade the system's performance. A low level of solar radiation or shallow geothermal resources may not provide enough benefits to offset the costs. Moreover, weather conditions and location can limit the effectiveness of solar-geothermal heat pump coupling.

Table 2
Overview of GSHP studies.

Reference	Purpose	Refrigerant	Type of analysis	Concluding remark
Liu et al. [89]	Heating	N/A	Energy/Simulation	The use of an auxiliary heat source in the GSHP can stabilise the performance for an extended period.
Maddah et al. [86]	Heating	R134a, R125, R404A, R407C, and R410A, R507A	Energy, exergy and economic/Experimental	The GSHP with R134a has a higher energy performance than an ASHP. It reduces electricity consumption by 239 MWh.year^{-1}, CO_2 emissions by 140 tons per year, and operating costs by 27,280 $ per year.
Akbulut et al. [87].	Heating	R410A	Energy, exergy, exergoenvironmental, and exergoeconomic/Experimental and simulation	The proposed system demonstrates a higher performance and lowers the fuel consumption, with energy and exergy efficiencies of 67.4% and 27.4%, respectively.
Cui et al. [90]	Heating and cooling	N/A	Energy/Simulation	Coupling with a cooling tower reduced the injected water temperature. The parallel configuration was stable, with a fixed temperature across the heat pump.
Ozyurt and Ekinci [22]	Heating and cooling	R134a	Energy/Experimental	The system can be efficiently used for residential heating in the coldest climate regions, with a COP ranging from 2.4 to 3.6.
Hepbasli et al. [85]	Heating and cooling	N/A	Energy/Experimental	The system's overall COP was lower than that of a conventional heat pump because the components were oversized.
Cho and Min Choi [91]	Cooling and hot water	R134a	Energy/Experimental	The waste heat exchanger increased the cooling and heating capacity and COP compared with a traditional system.
Liu et al. [92]	Heating and cooling	R410A	Energy/Experimental	The system performed better in terms of cooling than the conventional air-source heat pump system, with the cooling capacity being improved by 4.6% to 31.1% and the system COP being improved by 35.6% to 59.5%.

5. Data centre waste heat

5.1. Background

Indoor conditions strongly influence the performance and lifetime of electronic components in data centres; thus, the performance of the cooling system represents a crucial operational challenge [111]. A cooling system typically releases excess heat into the ambient environment to prevent damage to the components and to ensure a good performance [112]. To overcome the data centre's thermal load, the cooling system consumes 40% of the total power consumed by the entire facility [27].

A few studies have highlighted the reuse of waste heat produced by data centres using different configurations (Fig. 14). He et al. [113] proved that using heat pipe–heat pump arrangements in data centre cooling for supporting district heating networks (DHN) would save energy consumption by 10% compared with traditional coal boilers. Sheme et al. [114] concluded that combining renewable sources with data centre cooling provided more significant surplus hours than when using the systems alone. Deymi et al. [115] showed that using an air-based, water-based, and/or combined air or water economiser for data centres would reduce the cooling requirements by 80%. Oró et al. [116] observed that an air-to-water heat exchanger in a data centre's indoor air return duct shows promising thermo-economic results. Wahlroos et al. [117] showed that a high utilisation of the waste heat produced by the data centre in DHNs could save costs up to 7.3%. Oró et al. [118] proposed using liquid cooling on-chip servers' configuration waste heat for a swimming pool. Waste heat utilisation reduces power consumption by 6% compared with a traditional air-cooling type system, with a 60% reduction in CO_2-eq emission. In the same context, Fig. 14 presents two different waste heat recovery technologies, Fig. 14.a in this arrangement; the Data centre waste was recovered and upgraded to a district heating network required level using a combined heat pump-PV/T waste heat with the evaporative condenser as a full ejector driving force, avoiding an ejector pump need. On the other hand, the system shown in Fig. 14.b used supplementary ASHP with the chiller unit to recover the Data centre waste and upgrade it to a district heating network required level.

From the studies summarised in Table 4, it can be concluded that the data centre's waste heat utilisation for heating reduces greenhouse gas emissions because the natural gas is conserved. Several systems were proposed in these reviewed studies. Most studies have focused on thermal performance without considering the side effects of refrigerants with high GWP.

5.2. Data centre waste heat summary

One of the key challenges in managing data centre waste heat is its low temperature, which makes it difficult to recover and reuse effectively (the water chiller evaporator is in the range of (2 to 6 °C), so using it as an evaporator heat source will not bring more augmentation on overall cooling system performance, therefor combining with other techniques (ejector, heat pipe, and evaporative cooling) is mandatory to increase the cooling system performance. Integrating heat pipes into a

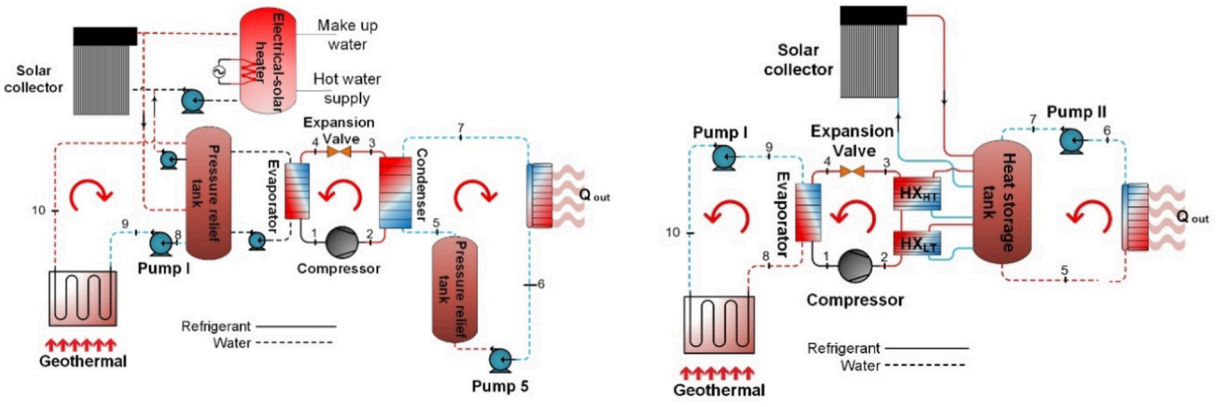

Fig. 12. SAGSHP configurations. Adapted from: (a) Trillat-Berdal et al. [99], and (b). Kim et al. [95].

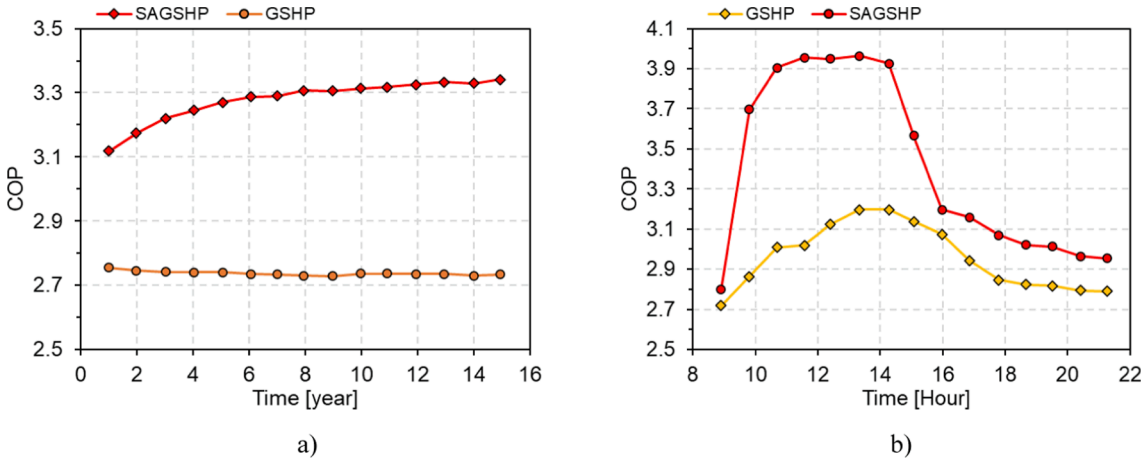

Fig. 13. Comparison of the performance of SAGSHP and GSHP at different operating periods: a) adapted from Wang et al. [100], and b) Yang et al. [96].

Table 3
Overview of SAGSHP studies.

Reference	Purpose	Refrigerant	Type of analysis	Concluding remark
Ozgener et al. [101]	Greenhouse heating	R22	Energy/Experimental	The system's COP was 5% to 20% lower than that of a traditional heat pump. For very-low ambient temperatures, the system should be combined with another heating system to overcome the overall heat loss of the greenhouse.
Ozgener et al. [102]	Greenhouse heating	R22	Exergy/Experimental	The COP of the GSHP and the overall system were 2.6 and 2.4, respectively, while the overall exergy efficiency was 67.7%. The greenhouse fan-coil unit represents the largest source of exergy destruction, followed by the compressor and condenser.
Trillat-Berdal et al. [103]	Domestic hot water, heating, and cooling	Water	Energy/Experimental	The average heating COP of the heat pump was 3.8. The combination of the thermal solar collectors can reduce the number of boreholes and the investment cost of the system installation.
Yang et al. [96]	Heating	N/A	Energy/Simulation	Compared with a GSHP, the developed system showed a 14.5% and 10.4% reduction in the energy consumption with and without a water tank, respectively.
Wang et al. [98]	Heating and cooling	R22	Energy/Experimental and simulation	Solar energy covered 49.7% of the total heating demand. In the heating mode, the heat pump's COP and overall COP were 4.3 and 6.6, respectively. In the cooling mode, the heat pump's COP was 2.1.
Bakirci et al. [104]	Heating	N/A	Energy/Experimental	The heat pump's COP and overall COP were in the range of 3.0 to 3.4 and 2.7 to 3.0, respectively. The system was economically preferable over the LPG, electricity, and fuel oil.
Chen and Yang [105]	Space heating and domestic hot water	N/A	Energy/Simulation	Solar energy can provide 75% of the hot water requirement, and the system is more efficient and economical for the Beijing area.
Rad et al. [106]	Heating	Water	Energy and economic/ Simulation	The developed system presented a moderate economic benefit (3.7–7.6%) compared with a conventional GSHP system.
Kim et al. [95]	Heating	CO_2	Energy/Simulation	The combination of the heat pump with solar and geothermal sources has an improving effect and increases the system's ability to meet the heat demand during winter.
Zheng et al. [107]	Heating and cooling	N/A	Energy and economic/ Simulation	The combined system saves more than 43% energy compared with an ASHP. The combined GSHP–ASHP system demonstrated optimum energy and economic parameters.
Ma et al. [108]	Heating	R22	Energy/Experimental	The system demonstrated heating stability by overcoming the shortcomings of solar energy and a higher heat-pump performance by increasing the evaporating temperature and the efficiency of the solar collector.
Chen et al. [109]	Heating, cooling, and power	R134a	Energy, exergy, and economic/Simulation	The system's energy and exergy efficiencies were higher than those of a conventional GSHP, with a 46% reduction in CO_2 emissions and an annual cost saving of 14.3%.
Kim et al. [110]	Heating, cooling, and domestic hot water	N/A	Energy/Simulation	The system has the highest COP of 4.56, with power savings of 13 and 19%, compared to air and geothermal source heat pumps.

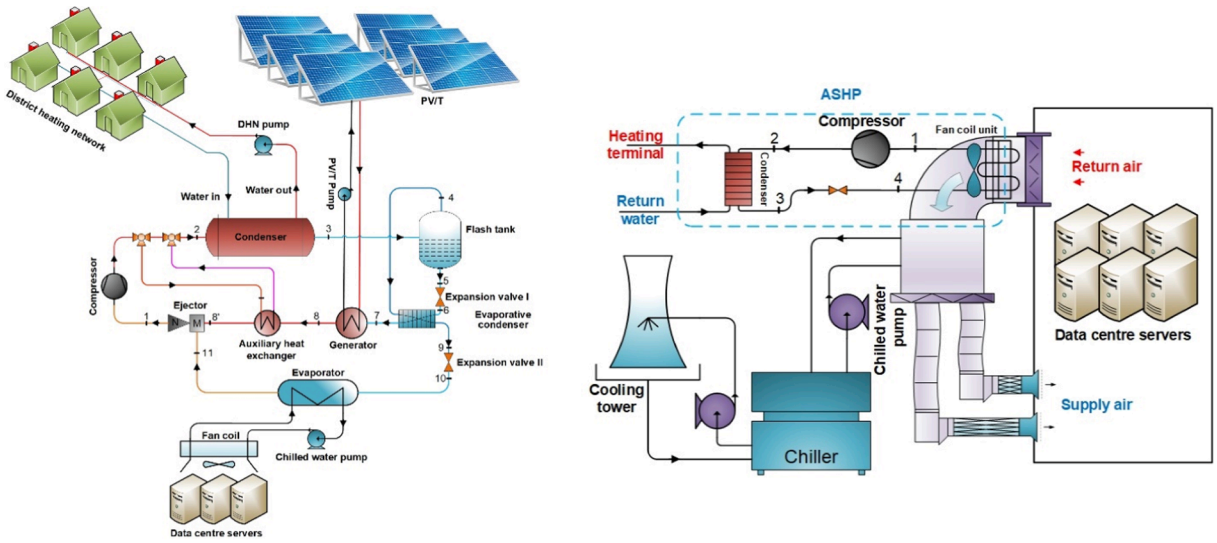

Fig. 14. Proposed data centre cooling systems. Adapted from (a) Al-Sayyab et al. [119] and (b) Deymi et al. [120].

data centre cooling system improves the overall performance owing to the extraction of higher waste heat and reduced power consumption. Ejector coupling with the data centre cooling system reduces compressor power consumption for overall cooling system and data centre performance. Using data centres' waste heat in absorption refrigeration systems benefits economic and environmental parameters. A VCC with evaporative or free cooling reduces power consumption by reducing the operating period of the cooling system. In spite of these efforts, much remains to be done to fully utilise data centre waste heat. In order to manage this valuable resource efficiently and effectively, more research and development are needed.

6. Combination with organic Rankine cycle and renewable energy sources

6.1. Background

ORCs have emerged as promising technologies for recovering low-grade thermal energy owing to their several advantages, including simplicity, the use of non-corrosive moderate-pressure working fluids, and low-cost component materials. Furthermore, it can be used in small-scale power [128,129]. All these reasons make it is being adopted.

The European service sector (heating and cooling) will need 40% more electricity by 2030 than that in 2012 [130]. Thus, one of the biggest challenges for the future is to produce green electricity while investing in highly efficient cooling systems.

The growing interest in the use of efficient energy has led to the development of trigeneration technologies (cooling, heating, and power generation). ORC and heat pumps or refrigeration systems can be combined to improve the overall performance of both systems. ORCs and VCCs (ORC-VCC) can be combined through a turbine–compressor mechanical or non-mechanical (electrical) coupling.

In mechanical coupling, the system demonstrates flexibility with an unmixed working fluid stream (dual or single fluid) and, in some cases, utilises the waste heat generated from the VCC condenser. The main disadvantages of this system are the low overall performance [131], ORC net power generation (because turbine expansion and rotation speed are limited), and, in some cases, power consumption by the VCC compressor for operating the compressor [132]. The COP of the system was limited and did not exceed unity (the system's COP was obtained by multiplying the ORC thermal efficiency with the VCC's COP) [133]. Most studies focused on new multi-purpose systems without accounting for the overall results and only considering a straightforward configuration.

In non-mechanical coupling, electric power generation was used to run the VCC compressor. The ORC and VCC subsystems are combined through a condenser, evaporator (cooling or heating), or flash tank [134], and can operate using a single or dual fluid according to the system arrangement requirement. This results in higher system performance with more net power generated owing to the operational flexibility of the turbine [135]. The disadvantages are complexity, more than three heat exchangers required (for instance, Molés et al. [136] considered 7), maintenance and initial cost.

Another non-mechanical coupling proposed for the ORC–refrigeration system combination is an ejector refrigeration cycle (ORC-ERC) that uses the expansion of the refrigerant through the ORC's turbine as the ejector driving force or shares the ORC's condenser waste heat source heat exchanger. Nevertheless, the ERC always had a lower COP than the vapour compression system, and the combined system exhibits a low overall performance [137]. Finally, ORC can be combined with an absorption refrigeration cycle (ARC), wherein these systems are combined through non-mechanical coupling using a waste heat–source heat exchanger.

6.2. Technologies applied for combining the ORC systems and renewable sources

Given the different technologies applied for combining the ORC systems and renewable sources, the rest of the section is divided according to the different combinations mentioned previously: ORC and vapour compression cycle (ORC-VCC), ORC and absorption refrigeration cycle (ORC-ARC) and ORC and ejector refrigeration cycle (ORC-ERC), different ORC coupling methods are showing in Fig. 15.

6.3. ORC and vapour compression cycle (ORC-VCC)

Using ORC with vapour compression heat pumps can transform the energy sector as a revolutionary idea. Combining these two technologies creates a robust system that converts waste heat into valuable energy.

A few studies have investigated the combination of an ORC with vapour compression heat pumps (ORC-VCC) for individual energy-efficient cooling and power or heating and power purposes. Molés et al. [136] simulated an ORC-VCC configuration using R1336mzz(Z) as the ORC working fluid and presented a slightly high electrical efficiency but moderate thermal efficiency. Yu et al. [138] concluded that ORC-VCC does not always improve the overall performance. A few studies

Table 4
Overview of data centre waste heat utilisation studies.

Reference	Configuration	Purpose	Refrigerant	Type of analysis	Concluding remark
Deymi et al. [120]	Combined chiller- heat pump	Cooling and heating	R134a, R410A, R404A and R407C	Thermoeconomic and environmental/ Simulation	The system with R134a demonstrated the highest increase in the system's COP from 5.2 to 5.5, with annual natural gas, electricity, and CO_2 emission savings of 35,000 m^3, 20.8 MWh, and 121 Ton, respectively.
Ebrahimi et al. [121]	Combined chiller-ARC	Cooling	R245fa, R245ca, water-ammonia, LiBr-water	Energy and exergy/ Simulation	The heat recovered from 3 to 5 racks can be used to operate an ARC to cool an additional rack.
Chen et al. [122]	Spray cooling-waste heat-ARC	Cooling	LiBr-water	Energy, exergy and economic/Simulation	The combined system met the cooling load demands during the peak time, with energy efficiency, exergy efficiency, and operational cost savings of up to 51%, 17%, and 71%, respectively.
Zhang et al. [123]	Water-cooled integrated AC with thermosyphon	Simultaneous heating and cooling	N/A	Energy/Simulation	Energy saving for simultaneous building cooling and heating, with more than 30% of power saving in the cooling mode compared with the conventional cooling system and more than 66% of power saving compared with the coal-fired boiler.
Deymi-Dashtebayaz et al. [124]	Combined free cooling-HP	Simultaneous heating and cooling	N/A	Energy, environment, economic/Simulation	Energy efficiency improvement of 16% and annual natural gas and CO_2 emission savings higher than 15,000 m^3 and 267 tons.
Han et al. [125]	Integrating HPi with ECACS	Cooling	N/A	Energy/Simulation	Power consumption was reduced by 31.3%, and the overall COP increased by 29.5% compared with a conventional air conditioning system.
Wang et al. [126]	Integrating HPi with HP	Cooling	R22	Energy/Experimental	The integrated heat pipe system improved the data centre's performance by 0.3 lower PUE than a conventional air conditioning system.
He et al. [113]	Integrating HPi with HP	Simultaneous heating and cooling	N/A	Energy/Simulation	The implementation of the heat pipe shows power saving in the data centre by 10%, and using district heating will save 18,000 tons per year of coal compared with traditional heating boilers.
Huang et al. [127]	Integrating HPi with HP	Simultaneous heating and cooling	N/A	Energy and economic/ Experimental	Heat pipes are beneficial for data centre cooling and district heating. The energy efficiency ratio in the heat recovery mode was 4.5 when the temperature of the hot water was 50 °C.

have focused on increasing the overall performance using components such as built-in evaporators [139], flash tanks [140], and condensers [141]. From Fig. 16.a, this system has non-mechanical coupling by sharing a condenser with a single fluid; in this arrangement, the system suffers from the limitation of turbine expansion ratio (high expansion ratio, high compressor pressure ratio), so a low overall system performance, while the system showing in Fig. 16.b adapted from Al-Sayyab et al. [142], presented a trigeneration system (ORC-compound ejector heat pump) that utilised the compound ejector-heat pump condenser waste associated with the ground heat source for power generation, contributing to an overall system performance increase. The ejector-compressor combination reduces compressor consumption power which enhances VCE COP. The surplus ground source water from the ORC evaporator is used to satisfy the heating demand. Moreover, two chilled water evaporators of different supply temperature levels are obtained to meet the cooling demand.

Other studies have focused on using refrigerants with a low GWP. Saleh [133] numerically investigated the performance of an ORC-VCC

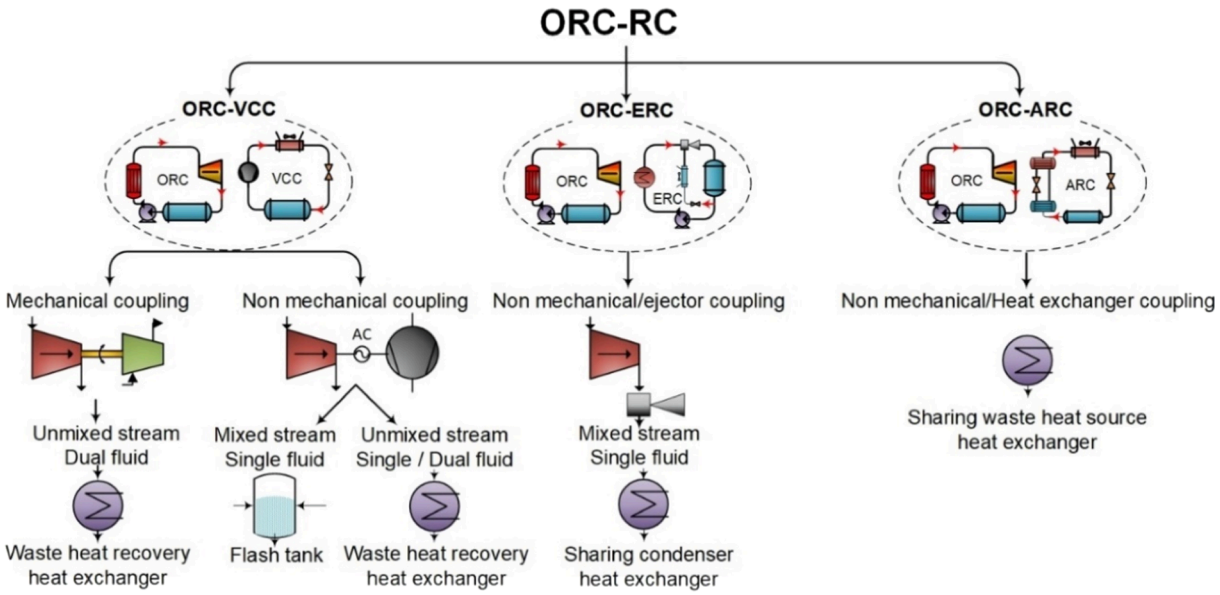

Fig. 15. Coupling methods for combining the ORC and the refrigeration system.

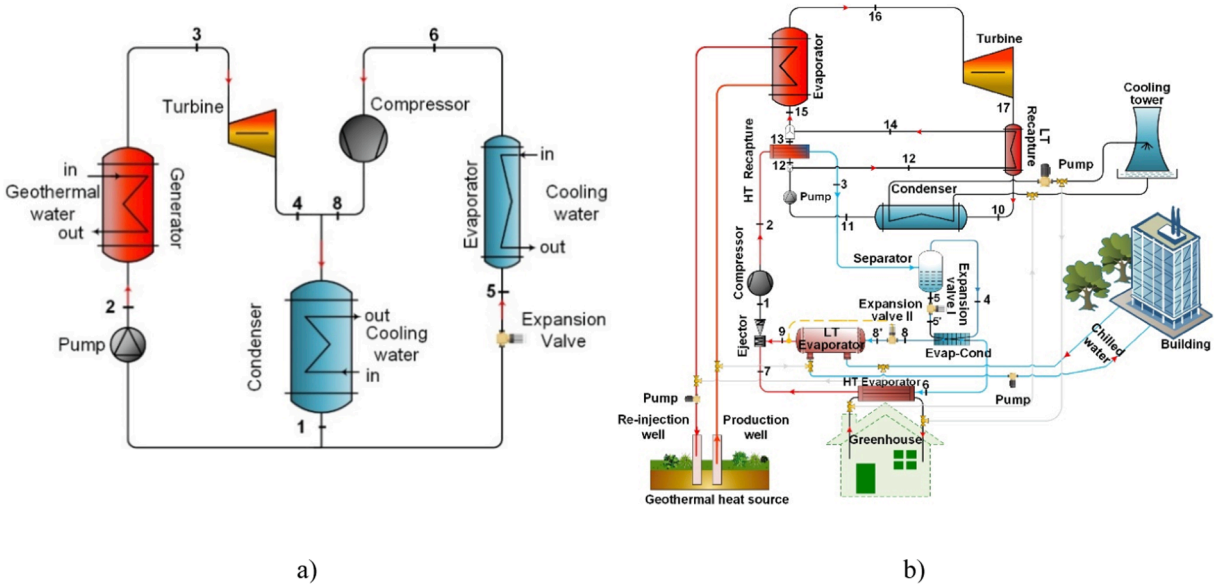

Fig. 16. ORC-VCC proposals. Adapted from: (a) Bao et al. [143], and (b) Al-Sayyab et al. [142].

powered by low-temperature renewable energy using R600, R600a, R601, R601a, R602, RC318, C5F12, R152a, R236ea, R236fa, R245ca, R245fa, RE245cb2, and R1234ze(E) as working fluids. The authors concluded that an increase in the condenser temperature decreased the performance, whereas an increase in the boiler temperature had the opposite effect. Few studies have focused on the use of dual and single fluids in the performance of ORC-VCC. Bao et al. [143] indicated that the dual fluid system performs better than a single fluid system.

Recently, a few studies have proposed the use of solar energy as the heat source of ORC-VCC. Zheng et al. [144] theoretically investigated five zeotropic mixtures and eight pure refrigerants as working fluids. Dry fluids demonstrated more advantages than wet fluids. R600a demonstrates the highest efficiency among the pure working fluids because of its high specific heat.

From the comparison between two different ORC-VCC couplings (mechanical and non-mechanical coupling with the condenser's waste heat), Fig. 17 shows that a higher evaporating temperature increases the COP. This highlights the increase in the COP with the non-mechanical coupling of the ORC-VCC owing to operational flexibility. In this system, the heat pump's performance was enhanced because of the reduced power consumption by the compressor (operating at a high evaporating temperature). Hence, using the condenser's waste heat increases the power generation of the ORC.

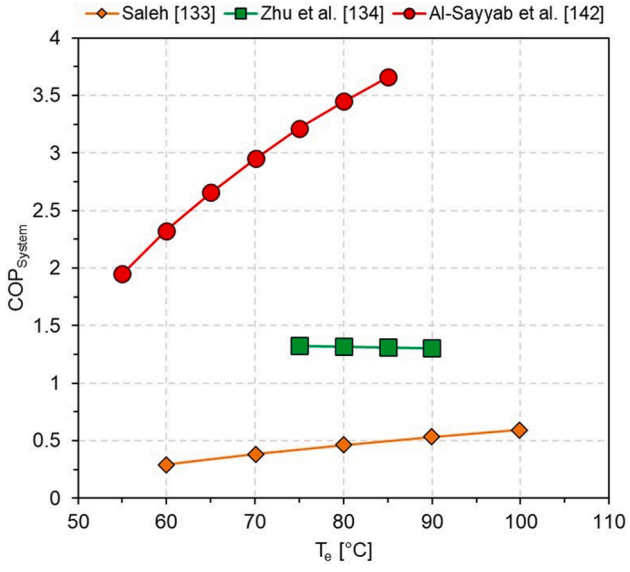

Fig. 17. COP for different ORC-VCC coupling versus evaporating temperatures. Values retrieved from Saleh [133], Zhu et al. [134], and Al-Sayyab et al. [142].

Table 5 shows that dual-fluid ORC-VCC systems always show the highest overall COP than the single-fluid systems owing to the beneficial thermal properties of the pair refrigerant.

The low GWP refrigerant R1234ze(Z) performs better than other studied refrigerants. Most studies focused on geothermal as an ORC heat source because it was the cheapest and most stable renewable energy source. In addition, other studies utilised the VCC condenser waste heat to augment the overall combined performance. Few studies considered ORC-VCC for trigeneration purposes, showing overall system performance increasing over many tested conditions. Increasing the variety of heat sources (waste heat or renewable energy) for the ORC increases the performance stability of the system and is recommended for future research.

7. ORC and absorption refrigeration cycle (ORC-ARC)

To avoid significant disasters, the world must reduce greenhouse gas emissions by 2030 and work towards carbon neutrality by 2050 [156]. The Montreal Protocol meeting parties approved a timeline for 65–85% reductions in HFCs by late 2040 [157]. Considering the environmental problems caused by vapour-compression systems, an alternative technology to replace conventional refrigeration systems is highly required. The Absorption Refrigeration Cycle (ARC) is a proven technology that utilises low-grade heat (solar energy and geothermal or waste heat) instead of electric power to operate the cycle. The generator and absorber act as thermal compressors [158]. Similar to other technologies, it has recently been combined with ORC; Fig. 18 incorporates the ORC-ARC coupling.

Studies have suggested utilising ORC waste heat as a source for ARC. Lu et al. [160] analysed an ORC-ARC combined system from the energy and exergy perspectives based on the waste heat generated by the boiler exhaust gas using different working fluids. The heat recovered from the waste heat recovery increased the energy and exergy efficiencies by 37.7% and 35.6%, respectively. Sun et al. [161] simulated a combination of the ORC-ARC and the R113 ejector refrigeration cycle (ERC) with waste heat from the flue gas. The proposed system exhibited better performance than the coupled system. Roumpedakis et al. [159]

Table 5
Overview of ORC-VCC studies (Continued).

Reference	Configuration	Purpose	Refrigerant	Heat source	Type of analysis	Concluding remark
Aphornratana et al. [145]	ORC-VCC	Cooling and power	R134a and R22	Waste heat	Energy/ Simulation	The R22 system had a higher COP than the R134a system. A liquid preheater decreased the generator heat energy input; therefore, the COP was increased.
Demierre et al. [146]	ORC-VCC	Heating and power	R134a	Geothermal	Energy/ Experimental	The compressor-turbine unit represents the main critical component. The evaporator and the pump are supercritical.
Molés et al. [136]	ORC-VCC	Cooling and power	VCC: R1234yf, R1234ze(E), and R134a. ORC: R1233zd(E), and R1336mzz(Z)	Waste heat	Energy/ Simulation	An increase in the VCC's evaporating temperature and a decrease in the ORC's condensing temperature increased the system's COP. The R1336mzz(Z)–R1234ze(E) pair demonstrated the highest thermal and electrical efficiency.
Akrami et al. [147]	ORC-hydrogen production	Heating, power and hydrogen production	R600a	Geothermal	Energy and exergy/ Simulation	The energy and exergy efficiencies were 26.1% and 44.5%, respectively. Net power generation and heating capacities were 43.5 kW and 149.8 kW, respectively.
Ebrahimi et al. [141]	ORC-VCC	Cooling and power	R134a-R245fa	Data centre	Energy and exergy/ Simulation	A higher waste heat temperature increased energy performance, whereas an increase in the ORC superheating and data centre cooling was detrimental. The payback period was between 4 and 8 years.
Yu et al. [138]	ORC-VCC	Cooling and power	R600a, R236ea, R600, R245fa, R123, R601, and n-hexane	Heat pump condenser waste heat	Energy/ Simulation	The combination system's net power generation increased by 9.4%, with an increase in waste heat recovery by 12%.
Saleh [133]	ORC-VCC	Cooling and power	R600, R600a, R601, R601a, R602, RC318, C5F12, R152a, R236ea, R236fa, R245ca, R245fa, RE245cb2, and R1234ze(E)	Waste heat	Energy and exergy/ Simulation	An increase in the evaporator and boiler temperature has an augmenting effect on system performance. The system condenser was the highest source of exergy destruction. The R602 system shows the highest energy and exergy performance.
Zheng et al. [144]	ORC-VCC	Cooling and power	R290, R161, R152a, R134a, R600a, R227ea, R1234yf, and R1234ze(E)	Solar	Energy and exergy/ Simulation	Binary mixtures showed higher performance than pure fluids. R290/ R600a/R161 (37.5/37.5/25% mass%) showed the highest thermal efficiency of 30.9%.
Javanshir et al. [148]	ORC-VCC	Cooling and power	R134a, R22, and R143a	Geothermal	Energy and exergy/ Simulation	R22 and R143a demonstrated the highest energy and exergy performance, while R134a showed the lowest performance. The boiler and turbine contributed the most to the total exergy destruction rate.
Liao et al. [149]	ORC-VCC	Heating, cooling and power	R227ea, R1234ze(E), R600, R245fa, R123, R601a, Hexane, Cyclohexane, and Heptane	Bottom slag waste heat in a coal-fired plant	Energy and exergy/ Simulation	The system's COP and refrigeration capacity were directly proportional to the chilled water mass flow rate. In contrast, the total exergy production rate was inversely proportional to the chilled water mass flow. The heptane-R601a pair shows the highest energy and exergy performance.
Pektezel and Acar [103]	ORC-VCC	Cooling and power	R134a, R1234ze(E), R227ea, and R600a	Water waste heat	Energy and exergy/ Simulation	The single evaporator configuration demonstrated a higher performance than the dual evaporator configuration. R600a presented a high system performance.
Bao et al. [143]	ORC-FTVIC ORC-VCC	Cooling and power	R1270, R1234yf, R290, R161, R1324ze(E), and R152a	Geothermal	Energy and exergy/ Simulation	The turbine inlet pressure, evaporation, and intermediate vapour injection temperature significantly influenced the cycle performance. R1234yf–R290 and R290–R152a pairs showed the highest performance.
Zhar et al. [150]	ORC-VCC	Cooling and power	R123, R11 and R113	Exhaust gases waste heat	Energy and exergy/ Simulation	R123 showed the highest energy and exergy efficiency of approximately 1.0% and 53%, respectively.
Nasir [151]	ORC-VCC	Simultaneous heating, cooling and power	ORC: R245fa, M−Xylene VCC: R600a	Biomass waste heat	Energy and exergy/ Simulation	The overall exergy destruction and the heat capacity rate were directly proportional to the boiler saturation temperature. The system can deliver 30 kW of cooling and 528 kW of heating.

(*continued on next page*)

Table 5 (*continued*)

Reference	Configuration	Purpose	Refrigerant	Heat source	Type of analysis	Concluding remark
Li et al. [152]	ORC-VCC	Cooling and power	R290, R600, R600a and R1270	waste heat	Energy/ Simulation	The boiler's exit temperature, evaporation temperature, and expander and compressor isentropic efficiencies significantly influenced the overall COP. R1270 showed the highest performance.
Liang et al. [132]	ORC-VCC	Cooling and power	ORC:R245fa VCC:R134a	Internal combustion (IC) engine waste heat	Energy/ Experimental	The cooling capacity was 1.8 kW at 4 °C of evaporating temperature and 95 °C of hot water temperature. The overall heat-to-cooling efficiency was 18%.
Eisavi et al. [153]	ORC-VCC and PV/T	Power and water distillation	R245fa	Geothermal and PV/T waste heat	Energy and exergy/ Simulation	PV/T and ORC generated 43.4 kW and 33.3 kW, respectively. A total of 38.7 kW was consumed to distil 141 $m^3.d^{-1}$ of water.
Ashwni et al. [140]	ORC-FTVCC	Cooling and power	hexane, heptane, octane, nonane, and decane	Biomass and solar	Energy and exergy/ Simulation	Heptane demonstrated the highest performance, with a COP of 0.55 and an exergy efficiency of 4.2%. The solar collector and biomass burner showed the highest exergy destruction.
Liu et al. [139]	ORC-VCC	Heating and power	R601, R365mfc, R245ca, R1233zd(E), R1224yd(Z), R600, R600a, R114, and R290	Hot water waste heat	Energy, exergy and economic/ Simulation	The built-in evaporator increased the thermal efficiency and waste heat recovery efficiency by 6.4% and 1.2%, respectively. R1233zd(E) showed the highest thermal and exergy efficiency of 32.2% and 38.9%, respectively.
Grauberger et al. [154]	ORC-VCC	Cooling and power	R1234ze(E)	Engine coolant waste heat in diesel generator sets	Energy/ Experimental	An increase in the condensing temperature reduced the system's COP. The system had a thermal efficiency and COP of 7.7% and 0.56, respectively.
Al-Sayyab et al. [142]	ORC-CEMES	Heating, cooling and power	VCC: R1234ze(E), R1243zf, R1234yf ORC: R1234ze(Z), R1336mzz (Z), and R1224yd(Z)	Geothermal and condenser waste heat	Energy and exergy/ Simulation	Compared to traditional ORC and multi-evaporator systems, a combination of R1234ze(Z)-R1234ze(E) system presents an overall energy performance increase: generated power and cooling COP increased from 21% to 75% and 85%, respectively.
Al-Sayyab et al. [155]	ORC-VCE	Heating, cooling and power	R1234ze(E), R1234yf, and R1243zf	Geothermal and condenser waste heat	Energy and exergy/ Simulation	System arrangement using R1234ze(E) increases system COP by 18 % on average in the power-cooling mode. Besides, a low-temperature recapture heat exchanger for condenser waste heat recovery increases power generation by 58%.

analysed three different configurations of a combined ORC-ARC for using boiler flue gas's waste heat as the heat source. A higher flue-gas temperature decreased the exergy performance. The ORC-ARC exhibited a higher exergy performance than the ORC-VCC, highlighting its double expander configuration. Wang et al. [162] analysed a solar-driven combined ORC-ARC using R600a, in which a 15-kW waste heat source could generate 1 kW of electric power with a 6.3-kW cooling capacity. The ARC's COP was 0.8, and the overall exergy efficiency ranged from 56% to 74%.

From the studies summarised in Table 6, it can be concluded that, despite the ARC representing a promising technology that produces a cooling effect from renewable or waste heat, it is often hampered by two significant problems: large cooling unit sizes (which makes the system suitable for industrial applications) and a low COP, which leads to a low overall performance of the combined system. All these studies were theoretical, which refers to the requirement of high economic investment. Moreover, these studies focused on the waste heat utilised from the source or ORC's condenser without increasing the use of a variety of ORC heat sources. This refrigeration system can be used as an auxiliary cooling source for ORC-VCC configurations by utilising the waste heat generated from the ORC's condenser.

7.1. ORC and ejector refrigeration cycle (ORC-ERC)

Low-grade energy ejector air-conditioning or refrigeration cycles (ERC) have been used since the mid-1950 s. Generators can be driven

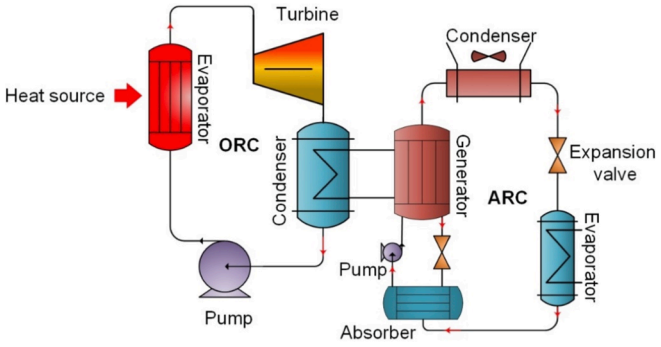

Fig. 18. Combination of ORC and ARC. Adapted from Roumpedakis et al. [159].

using solar energy or waste heat [165]. ERC have several advantages over other heat-driven refrigeration systems, including high reliability, simplicity, operation using low-grade waste heat, and low cost [166]. In general, the ERC consists of an ejector, condenser, ejector pump, expansion valve, and evaporator, whereas some systems also include flash tanks use solar energy as a driving force with a generator. The ejector and the pump were combined to replace the compressor. The combination of an ERC with an ORC can result in a cooling and power

Table 6
Overview of ORC-ARC studies.

Reference	Purpose	Refrigerant	Heat source	Type of analysis	Concluding remark
Xue et al. [163]	Simultaneous heating, cooling, and power	R601	Liquid air energy storage	Energy and exergy/ Simulation	The system showed a heating, cooling, and power generation of 1.8, 0.9, and 11.5 MW, respectively. Liquefaction, throttling, and regasification processes were the largest exergy destruction sources.
Li et al. [164]	Heating, cooling, and power	CO_2, LiBr-H_2O	Flue gases waste heat	Exergoeconomic/ Simulation	The system configuration showed an enhancement in the exergy efficiency and levelized cost of exergy by 4.62% and 0.90 % than that of a conventional power cycle.
Lu et al. [160]	Cooling and power	R245fa, R245ca, R236ea, R600, R601m, and R601a	Boiler exhaust gas waste heat	Energy and exergy/ Simulation	The waste heat recovery heat exchanger increased the energy and exergy efficiency by 37.7% and 35.6%, respectively, with a payback period of 4.6 years. Maximum electric power generation occurred when using R600a.
Sun et al. [161]	Cooling and power	R113-LiBr	Flue gas waste heat	Energy and exergy/ Simulation	Higher ORC evaporation temperatures decreased the exergy efficiency. The uncoupled ORC-ARC showed a higher performance than the ORC-ERC.
Roumpedakis et al. [159]	Cooling and power	R600, R114, R245ca, R245fa, Isohexane, and cyclopentane	Flue gas waste heat	Energy and exergy/ Simulation	The low pinch point of the ORC heat exchangers/flue gas increased the exergetic efficiency. ORC-ARC showed less exergy destruction and performed better than the combined ORC-VCC systems.
Wang et al. [162]	Cooling and power	R600a-silica gel water	Solar	Energy and exergy/ Simulation	For heating temperature of 97 °C and 15 kW heating power, the system can generate 1 kW electricity with 6.4 kW refrigeration capacity. The ARC has COP of 0.8, while overall exergy efficiency ranged from 56% to 74%.

generation system with fewer components (heat exchangers and pumps). Fig. 19 incorporates the concept of an ejector refrigeration system with ORC.

To date, only a few studies have considered ORC-ERCs and used solar and geothermal heat to increase the stability of the heat source. Boyaghchi et al. [167] evaluated an ORC-ERC for refrigeration and power generation combined with a geothermal source heat exchanger and a flat-plate solar collector. The exergoeconomic performance of the system was the highest when R1234yf was used. Tashtoush et al. [168] evaluated an R134a-combined ORC-ERC, in which the total exergy efficiency and the COP of the ERC were 20% and 0.53, respectively. Wang et al. [169] showed that the COP and cooling capacity of the ERC were 0.12 and 93.7 kW, respectively.

From the studies summarised in Table 7, it can be concluded that most studies focused on utilising the refrigerant pressure after turbine expansion as the ejector-driven force in the absence of the pump and using the ORC's condenser as the combined system condenser. This configuration leads to a reduction in the number of components and is economically beneficial compared with traditional ORC and ejector refrigeration systems. Both the ORC and ERC show low thermal performance (COP lower than unity), and their combination always leads to lower overall performance [164]. This type of combination is limited to a single fluid without taking advantage of the dual-fluid properties and is limited for cooling and power purposes. The working fluid is always limited to the operating conditions of a low heat-source temperature owing to the low critical temperature of the refrigerant. The advanced configuration of the ORC and ERC combined by the condenser's waste heat with dual fluids did not show a remarkable increase in the system performance. More attention should be paid to increasing the COP of the ERC by coupling it with other high-performance cooling systems, such as VCC.

7.2. Comparison of ORC-Refrigeration system coupling techniques

The ORC-refrigeration system coupling has been a topic of interest in recent years due to the potential for increased energy efficiency—both types of coupling: non-mechanical and mechanical, have advantages and disadvantages. Fig. 20 presents a comparison of the maximum ORC-refrigeration system COP of different studies; Fig. 20 indicates that non-mechanical coupling of ORC-VCC systems showed the highest COP owing to the flexibility of the turbine and compressor operating

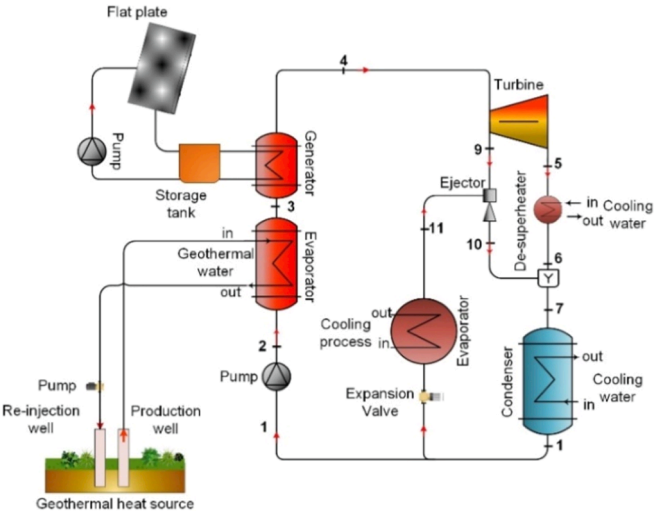

Fig. 19. Combination of ORC-ERC. Adapted from Boyaghchi et al. [167].

conditions (higher turbine expansion ratio and low compressor compression ratio) and the benefit of dual-fluid properties in some cases. In addition, Ebrahimi et al. [141] reported a stable and higher overall system performance owing to the enhanced subsystem performance of the vapour compression refrigeration system (reducing the compressor's work by increasing the evaporating temperature). In addition, Al-Sayyab et al. [142] indicated a notable higher overall system performance owing to the enhanced subsystem performance of the compound ejector-compressor refrigeration system (reducing the compressor work by compressor suction pressure increasing). The ORC performance increased when the heat pump condenser waste heat (additional heat source) was considered. The ARC is not included in Fig. 20 because of its low COP (less than 0.02).

Table 8 lists previous studies that have studied the combination of ORC and refrigeration systems. From Table 8, we can observe that non-mechanical coupling does not always increase the overall performance, which depends on the characteristics of the subsystem. In fact, the ORC's subsystem decreases its thermal efficiency to increase the overall

Table 7
Overview of ORC-ERC studies.

Reference	Purpose	Refrigerant	Heat source	Type of analysis	Concluding remark
Boyaghchi [167]	Heating, cooling and power	R134a, R423A, R1234ze(E) and R1234yf	Geothermal and solar	Energy, exergy, environmental and economic/Simulation	The system with R134a shows the best performance, with a daily exergy efficiency of 4.2%. In comparison, the system with R1234yf demonstrated better exergoeconomic performance.
Boyaghchi et al. [170]	Cooling, heating and power	ORC: R245fa, R236fa, R600 ERC: R134a, R1234yf, R290.	Biomass gasification	Energy, exergy, economic, exergoeconomic and exergoenvironmental/Simulation	The pair of R245fa–R134a showed the highest reduction in the total cost (39.5%), while the R236fa–R1234yf resulted in the highest environmental benefit (34.7%).
Saini et al. [131]	Heating, cooling and power	R600	Solar	Energy, exergy, environment, and economic/Simulation	An increase in the evaporating temperature benefitted the exergy efficiency, cooling, and power cost. A higher condensing temperature decreased the exergy efficiency, heating cost, and CO_2 emissions, although it decreased the cooling and power costs.
Du et al. [171]	Cooling and power	R245fa	Geothermal	Energy, exergy/Simulation	A higher condensing temperature decreased the net power generation. A higher evaporating temperature benefitted the cooling capacity and thermal efficiency.
Ahmadi et al. [172]	Cooling and power	R123	Gas turbine waste heat	Energy, exergy, and environmental/ Simulation	A higher gas turbine inlet temperature, compressor pressure ratio and ORC extraction pressure increased the system performance. Lower exergy destruction minimised the effect on the total cost rate.
Dai et al. [173]	Cooling and power	R123	N/A	Energy and exergy/Simulation	Turbine inlet and back pressures and condensing and evaporating temperatures significantly affected the power output, refrigeration output, and exergy efficiency. The maximum exergy efficiency was 27.1%.
Tashtoush et al. [168]	Cooling and power	R134a	Solar	Exergy, economic and exergoeconomic/Simulation	The solar subsystem showed the highest exergy destruction, followed by the ERC's condenser, ORC's condenser, and ejector. The total exergy efficiency was 20%, with a 0.53 ERC's COP.
Wang et al. [169]	Cooling and power	Mixture of R601/ R142b, R601a/R600a, and R601/R142b	Geothermal	Energy and exergy/Simulation	The mixture of R601/R142b with a mass fraction of (0.3/ 0.7) showed the highest system energy performance and low exergy destruction, with thermal and exergy efficiencies of 18.2% and 59.2%, respectively. The ERC's COP and cooling capacity were 0.12 and 93.7 kW, respectively.
Sanaye et al. [174]	Cooling and power	ORC: Toluene ERC: R600a	Engine exhaust gas	Energy and exergy/Simulation	The system has the ability to produce 271.1 kW of cooling capacity, 0.33 of COP, and 225.6 kW of power output, with a 26.2% of thermal efficiency. The system payback period is approximately 2.7 years.
Zhao et al. [175]	Cooling and power	R245fa	Geothermal	Exergoeconomic/Simulation	The system performance was affected by the flash pressure, vapour generator, pinch point temperature difference, inlet pressure, and ORC's turbine pressure.
Yang et al. [176]	Cooling and power	Mixture R600a/R601	Hot air	Energy and exergy/Simulation	The system showed a higher energy and exergy performance at lower condensing and higher generating temperatures. The system with a mixture of isobutane/ pentane (70%/30%) by mass shows a maximum thermal efficiency of 10.8%.
Zhu et al. [134]	Heating, cooling and power	Mixture R141b/R134a	Geothermal	Energy and exergy/ Simulation	The blend of R141b/R134a (55%/45%) by mass fraction obtained a higher system performance than pure R141b or R134a, with 4.2% power efficiency and system COP of 1.1.

performance. ORC should be coupled with a high-performance refrigeration subsystem such as vapour compression technologies. This explains why the non-mechanical coupling of ORC with ERC has deficient overall performance, as in the non-mechanical coupling of ORC with ARC. Of note, the proposed system by Lu et al. [160] presented the highest thermal efficiency owing to using a steam power plant as the subsystem.

7.3. ORC-Refrigeration system coupling summary

The following inferences were made regarding the present section: First, when an ORC is combined with an ARC, the overall system exhibits a low overall performance and requires a large space for implementation. Second, an ORC combined with an ERC has the disadvantage of low system performance but limited single working fluid and cooling and power purposes. Moreover, many studies are based on simulation, allowing continual laboratory verification and industrial production. Finally, an ORC combined with a VCC is highlighted because of its significant overall performance, representing a technology that can be implemented in industrial applications.

Several actions can be implemented to extend the application possibilities of ORC-VCC: increasing the waste heat sources to increase the stability, using phase-change materials as waste heat storage batteries, and combining them with PV/T panels as an auxiliary electric source. Additionally, combining ORC with a compound ejector–heat pump can represent a promising design for power generation and simultaneous heating and cooling. In addition to the economic and environmental benefits of the ejector, the VCC condenser's waste heat will increase the generated power to reduce greenhouse gas emissions.

8. Conclusions

Renewable (solar and geothermal sources; individual and combined), data centre waste heat, and ORC technologies have been considered to improve the energy performance of heat pumps owing to renewable and waste heat utilisation. The objective of this study was to comprehensively review the heat pumps combined with other clean technologies for power generation, heating, and/or cooling. Different

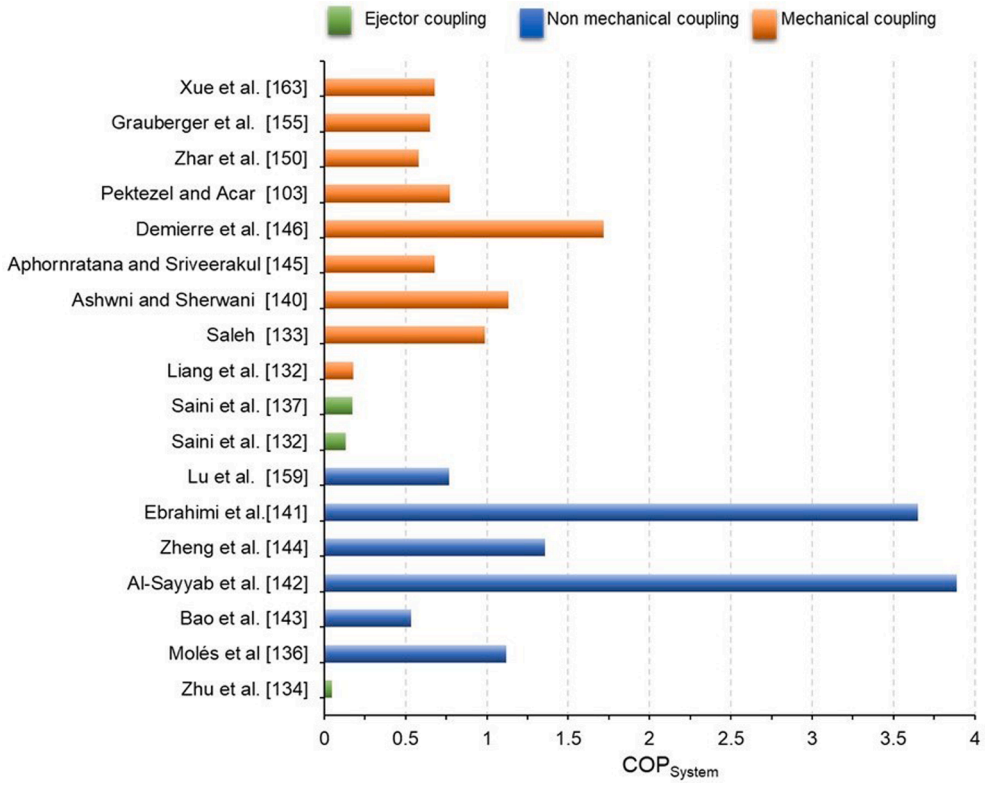

Fig. 20. Maximum ORC-refrigeration system COP for different studies.

system configurations were investigated considering the theoretical and experimental approaches from the energy, exergy, environmental and economic perspectives to determine the possibilities of these advanced systems in different applications. The main conclusions of this study are as follows:

SAHPs can improve the system's performance. These can be combined with a storage tank or phase-change materials to address the absence of sunlight and fluctuations in weather conditions. However, this proposed system is still inefficient for prolonged periods in contrast to the weather conditions or fluctuations. The compound ejector-SAHP improved the system performance by reducing the compressor power consumption and increasing the system's COP.

Various heat sources can overcome the thermal imbalances encountered in conventional geothermal-assisted heat pumps and SAHPs. Geothermal-source solar-assisted heat pump systems can exhibit stable, continuous performance with high annual overall performance compared with other configurations. This can be achieved by combining geothermal and solar sources, extending the variety of waste heat sources (data centres and sewage water) used, or modifying the PV/T coil design and combining it with heat pipes. In addition, using a phase-change material storage tank can increase the system's stability.

A multi-function–combined multi-source heat-driven ejector heat pump (simultaneous cooling, heating, and power generation) represents a promising technology. Increasing the energy performance of this type of system is essential for its widespread use. Additionally, the system can be coupled with other residential, commercial, or industrial applications with excessive heating or cooling demands.

Compared with basic ORC configurations, a dual-fluid ORC-VCC with the condenser's waste heat can produce simultaneous heating, cooling, and power generation with high overall performance. More attention should be paid to increasing the COP of the ORC-ERC by coupling it with other high-performance cooling systems, such as VCC.

Combined ORC-ARC systems represent a green cooling and power generation technology but have a low system performance and require large space for installing the system. By contrast, non-mechanical ORC–VCC coupling provides operating flexibility under different conditions with high system performance. Using the waste heat of the ORC-VCC's condenser to drive the ARC as a supplementary cooling system can reduce the required power consumption.

9. Future directions for heat pump coupling research and development

Integrating HP into innovative systems has already taken a lot of effort, but much more is still needed. Multi-purpose simultaneous cooling, heating and power generation represent a promising technology, which presents an integrated system with high performance, energy-saving and CO_2-eq emissions reduction. Several future-proof technologies are combined, including PV/T, ejector-heat pump, and waste heat utilisation. This solution caused an overall air conditioning system performance enhancement and remarked energy-saving and CO_2-eq emissions reduction.

After conducting a thorough review of integrating HP into different renewable and waste heat, the author would like to highlight suggested research lines directions for future research, which can be listed below:

- Increasing the variety of heat sources (waste heat or renewable) to increase the performance stability of the system over an extended period of operation.
- Performing multi-objective optimisation for compound system components.
- Investigating the ORCs coupled with multi-ejectors and compound vapour compression systems under different conditions.
- Developing an ejector-compound vapour compression system for ultra-low temperature applications.
- Using eco-environmentally friendly refrigerant with GWP below 150.
- Advancing a multi-stage ORC with multi-renewable and waste heat sources.

Table 8
Summary of ORC and refrigeration cycle combination studies.

Reference	Subsystem coupling			No. of HXs	Maximum net power [kW]	Thermal efficiency	Maximum COP_{system}
	Compressor/Turbine or expander	Heat exchanger shared	Other				
Molés et al. [136]	Non-mechanical, generated power partially used for heat pump operation	Condenser	VCC	7	16.3	15.0%	1.12
Yu et al. [138]	Non-mechanical, generated power partially used for heat pump operation	Condenser	VCC	3	805	10.1%	N/A
Bao et al. [143]	Non-mechanical	Condenser	VCC	3	N/A	N/A	0.54
Al-Sayyab et al. [142]	Non-mechanical	Condenser	VCC	7	348	35.0%	3.89
Zheng et al. [144]	Non-mechanical	Condenser	VCC	3	28	27.6%	1.36
Ebrahimi et al. [141]	Non-mechanical	Condenser	VCC	3	N/A	10.0%	3.65
Javanshir et al. [148]	Non-mechanical	Condenser	VCC	4	1800	32.2%	N/A
Zhar et al. [150]	Non-mechanical	Condenser	VCC	3	0	10.8%	0.58
Liu et al. [139]	Mechanical	Evaporator	VCC	3	N/A	32.2%	N/A
Ashwni and Sherwani [140]	Mechanical	Condenser	VCC	4	N/A	N/A	1.13
Saleh [133]	Mechanical and mixing chamber	Condenser	VCC	3	N/A	53.8%	0.99
Aphornratana and Sriveerakul [145]	Mechanical	Condenser	VCC	4	N/A	N/A	0.68
Demierre et al. [146]	Mechanical	Condenser	VCC	4	N/A	N/A	1.72
Liao et al. [149]	Mechanical and mixing chamber	Condenser	VCC	5	N/A	19.4%	N/A
Pektezel and Acar [103]	Mechanical	N/A	VCC	5	N/A	N/A	0.78
Nasir et al. [151]	Mechanical	N/A	VCC	7	100	N/A	N/A
Liang et al. [132]	Mechanical	N/A	VCC	4	0	N/A	0.18
Grauberger et al. [154]	Mechanical	N/A	VCC	7	N/A	8.1%	0.65
Lu et al. [160]	Non-mechanical power generated partially used for ARC pumps operation	Condenser-generator	ARC	10	550	58.2%	0.77
Xue et al. [163]	Non-mechanical	Condenser	ARC	19	1230	N/A	0.68
Zhu et al. [134]	Non-mechanical refrigerant after condenser as the ejector-driven force	Separator tank	ERC	4	97	14.6%	1.12
Boyaghchi et al. [170]	Non-mechanical	Condenser	ERC	6	N/A	77.0%	N/A
Yang et al. [176]	Non-mechanical refrigerant after turbine expansion as the ejector-driven force	Condenser	ERC	3	141.3	N/A	N/A
Du et al. [171]	Non-mechanical refrigerant after ORC evaporator as an ejector-driven force	Condenser	ERC	3	97.2	10.7%	N/A
Zhao et al. [175]	Non-mechanical refrigerant after turbine expansion as an ejector-driven force	Condenser	ERC	4	271.2	14.6%	N/A
Saini et al. [137]	Non-mechanical refrigerant after turbine expansion as an ejector-driven force	Condenser	ERC	5	0.022	N/A	0.18
Saini et al. [131]	Non-mechanical refrigerant after condensing as an ejector-driven force	Condenser	ERC	5	0.105	12.9%	0.13
Ahmadi et al. [172]	Non-mechanical	Refrigerant after turbine expansion as an ejector-driven force	ERC	4	N/A	N/A	N/A
Dai et al. [173]	Non-mechanical		ERC	3	149.9	N/A	N/A
Tashtoush et al. [168]	Non-mechanical	Waste heat source	ERC	6	8.31	6.16%	0.032
Wang et al. [169]	Non-mechanical	Waste heat source	ERC	6	255	18.2%	0.022
Sanaye et al. [174]	Non-mechanical	Condenser	ERC	6	225.6	26.6%	0.33

- Several knowledge gaps need to be addressed to develop our understanding of ORC-refrigeration system coupling; further research is needed to determine which method is best suited for specific applications, so quantitative and qualitative comparison studies are required for mechanical and non-mechanical coupling.

Declaration of Competing Interest

The authors declare that they have no known competing financial interests or personal relationships that could have appeared to influence the work reported in this paper. Adrián Mota-Babiloni acknowledges grant IJC2019-038997-I funded by MCIN/AEI/10.13039/501100011033.

Data availability

The authors are unable or have chosen not to specify which data has been used.

References

[1] Kovats S, Menne B, Mcmichael A, Bertollini R, Soskolne C. Climate change and stratospheric ozone depletion Early effects on our health in Europe Contents; 2000.
[2] IEA (2021), Electricity Market Report - July 2021, IEA, Paris https://www.iea.org/reports/electricity-market-report-july-2021, n.d.
[3] EuropeanEnvironmentAgency, Renewable energy in Europe: key for climate objectives, but air pollution needs attention; 2019.
[4] U.S. Energy Information Administration, Renewable energy explained; 2020. https://www.eia.gov/energyexplained/renewable-sources/.
[5] ECMWF, Copernicus: 2020 warmest year on record for Europe; globally, 2020 ties with 2016 for warmest year recorded, in: 2020.
[6] European Heat Pump Association (EHPA), Heat pump record, 2022. https://www.ehpa.org/market-data (accessed March 5, 2023).
[7] Baxter V, Groll E, Sh B. Air source heat pumps for cold climate applications–Recent U. S. R&D results from IEA HPP Annex 41, REHVA J; September 2014.
[8] Khalifa AHN, Faraj JJ, Shaker AK. Performance study on a window type air conditioner condenser using alternative refrigerant R407C. Eng J 2017;21:235–43. https://doi.org/10.4186/ej.2017.21.1.235.
[9] European commission, Regulation of the European parliament and of the council 'on establishing the framework for achieving climate neutrality and amending'Regulation (EU) 2018/1999 (European Climate Law), 2020.

[10] Hewitt CN, Jackson AV. Atmospheric Science for Environmental Scientists. Wiley; 2020. https://books.google.es/books?id=CcrBDwAAQBAJ.

[11] Mota-Babiloni A, Makhnatch P, Khodabandeh R. Recent investigations in HFCs substitution with lower GWP synthetic alternatives: Focus on energetic performance and environmental impact. Int J Refrig 2017. https://doi.org/10.1016/j.ijrefrig.2017.06.026.

[12] Mota-Babiloni A, Navarro-Esbrí J, Makhnatch P, Molés F. Refrigerant R32 as lower GWP working fluid in residential air conditioning systems in Europe and the USA. Renew Sustain Energy Rev 2017;80:1031–42. https://doi.org/10.1016/j.rser.2017.05.216.

[13] The European Environment Agency (EEA), Fluorinated greenhouse gases 2021, 2021. https://www.eea.europa.eu/publications/fluorinated-greenhouse-gases-2021 (accessed April 3, 2022).

[14] United Nations, Report of the Twenty-Eighth Meeting of the Parties to the Montreal Protocol on Substances that Deplete the Ozone Layer, Twenty-Eighth Meet. Parties to Montr. Protoc. (2016) 72.Protoc 2016;72.

[15] Tagliafico LA, Scarpa F, Valsuani F. Direct expansion solar assisted heat pumps – A clean steady state approach for overall performance analysis. Appl Therm Eng 2014;66:216–26. https://doi.org/10.1016/j.applthermaleng.2014.02.016.

[16] Egilegor B, Jouhara H, Zuazua J, Al-Mansour F, Plesnik K, Montorsi L, et al. ETEKINA: Analysis of the potential for waste heat recovery in three sectors: Aluminium low pressure die casting, steel sector and ceramic tiles manufacturing sector. Int J Thermofluids 2020;1–2:100002. https://doi.org/10.1016/j.ijft.2019.100002.

[17] Brückner S, Liu S, Miró L, Radspieler M, Cabeza LF, Lävemann E. Industrial waste heat recovery technologies: An economic analysis of heat transformation technologies. Appl Energy 2015;151:157–67. https://doi.org/10.1016/j.apenergy.2015.01.147.

[18] Law R, Harvey A, Reay D. Opportunities for low-grade heat recovery in the UK food processing industry. Appl Therm Eng 2013;53:188–96. https://doi.org/10.1016/j.applthermaleng.2012.03.024.

[19] Yao Y, Jiang Y, Deng S, Ma Z. A study on the performance of the airside heat exchanger under frosting in an air source heat pump water heater/chiller unit. Int J Heat Mass Transf 2004;47:3745–56. https://doi.org/10.1016/j.ijheatmasstransfer.2004.03.013.

[20] A. Khalid Shaker Al-Sayyab, A. Mota-Babiloni, J. Navarro-Esbrí, Novel compound waste heat-solar driven ejector-compression heat pump for simultaneous cooling and heating using environmentally friendly refrigerants, Energy Convers. Manag. 228 (2021) 113703. https://doi.org/https://doi.org/10.1016/j.enconman.2020.113703.

[21] Li YW, Wang RZ, Wu JY, Xu YX. Experimental performance analysis and optimization of a direct expansion solar-assisted heat pump water heater. Energy 2007;32:1361–74. https://doi.org/10.1016/j.energy.2006.11.003.

[22] Ozyurt O, Ekinci DA. Experimental study of vertical ground-source heat pump performance evaluation for cold climate in Turkey. Appl Energy 2011;88:1257–65. https://doi.org/10.1016/j.apenergy.2010.10.046.

[23] Association GSM, Mobile economy Gsma 2020;2–62. https://www.gsma.com/mobileeconomy/wp-content/uploads/2020/03/GSMA_MobileEconomy2020_Global.pdf.GSM.

[24] E. Commission, I. Directorate-General for Internal Market Entrepreneurship and SMEs, S. Bayramoglu, N. Nissen, A. Berwald, T. Faninger, L. Stobbe, S. Mudgal, B. Tinetti, Ecodesign preparatory study on enterprise servers and data equipment, Publications Office, 2016. https://doi.org/doi/10.2873/14639.

[25] Avgerinou M, Bertoldi P, Castellazzi L. Trends in data centre energy consumption under the European code of conduct for data centre energy efficiency. Energies 2017;10. https://doi.org/10.3390/en10101470.

[26] GeSI. SMART 2020., enabling the low carbon economy in the information age, 2008. https://doi.org/10.1111/j.0906-7590.2007.04873.x.

[27] G. Payerle, R.C. Team, G. Payerle, S. D, S. Dolnicar, A. Chapple, A.W. Pastuszak, R. Wang, Report to congress on server and data center energy efficiency public law 109-431. public law 109, Ann. Tour. Res. 3 (2015) 45. http://www.ncbi.nlm.nih.gov/pubmed/25926610%5Cnhttp://www.pubmedcentral.nih.gov/articlerender.fcgi?artid=PMC4492060%0Ahttp://www.sciencedirect.com/science/article/pii/S0160738315000444.

[28] Lecompte S, Huisseune H, van den Broek M, Vanslambrouck B, De Paepe M. Review of organic Rankine cycle (ORC) architectures for waste heat recovery. Renew Sustain Energy Rev 2015;47:448–61. https://doi.org/10.1016/j.rser.2015.03.089.

[29] Meng N, Li T, Gao X, Liu Q, Li X, Gao H. Thermodynamic and techno-economic performance comparison of two-stage series organic Rankine cycle and organic Rankine flash cycle for geothermal power generation from hot dry rock. Appl Therm Eng 2022;200:117715. https://doi.org/10.1016/j.applthermaleng.2021.117715.

[30] Teng S, Feng YQ, Hung TC, Xi H. Multi-objective optimization and fluid selection of different cogeneration of heat and power systems based on organic rankine cycle. Energies 2021;14. https://doi.org/10.3390/en14164967.

[31] Mitsopoulos G, Syngounas E, Tsimpoukis D, Bellos E, Tzivanidis C, Anagnostatos S. Annual performance of a supermarket refrigeration system using different configurations with CO2 refrigerant. Energy Convers Manag X 2019;1:100006. https://doi.org/10.1016/j.ecmx.2019.100006.

[32] Chow TT, Pei G, Fong KF, Lin Z, Chan ALS, He M. Modeling and application of direct-expansion solar-assisted heat pump for water heating in subtropical Hong Kong. Appl Energy 2010;87:643–9. https://doi.org/10.1016/j.apenergy.2009.05.036.

[33] Mohanraj M, Muraleedharan C, Jayaraj S. A review on recent developments in new refrigerant mixtures for vapour compression-based refrigeration, air-conditioning and heat pump units. Int J Energy Res 2011;35:647–69. https://doi.org/10.1002/er.1736.

[34] Sun X, Wu J, Dai Y, Wang R. Experimental study on roll-bond collector/evaporator with optimized-channel used in direct expansion solar assisted heat pump water heating system. Appl Therm Eng 2014;66:571–9. https://doi.org/10.1016/j.applthermaleng.2014.02.060.

[35] Kong XQ, Li Y, Lin L, Yang YG. Modeling evaluation of a direct-expansion solar assistedheat pump water heater using R410A. Int J Refrig 2017;76:136–46. https://doi.org/10.1016/j.ijrefrig.2017.01.020.

[36] Fernández-Seara J, Piñeiro C, Alberto Dopazo J, Fernandes F, Sousa PXB. Experimental analysis of a direct expansion solar assisted heat pump with integral storage tank for domestic water heating under zero solar radiation conditions. Energy Convers Manag 2012;59:1–8. https://doi.org/10.1016/j.enconman.2012.01.018.

[37] Kong XQ, Zhang D, Li Y, Yang QM. Thermal performance analysis of a direct-expansion solar-assisted heat pump water heater. Energy 2011;36:6830–8. https://doi.org/10.1016/j.energy.2011.10.013.

[38] Del Amo A, Martínez-Gracia A, Bayod-Rújula AA, Cañada M. Performance analysis and experimental validation of a solar-assisted heat pump fed by photovoltaic-thermal collectors. Energy 2019;169:1214–23. https://doi.org/10.1016/j.energy.2018.12.117.

[39] Wang G, Quan Z, Zhao Y, Sun C, Deng Y, Tong J. Experimental study on a novel PV/T air dual-heat-source composite heat pump hot water system. Energy Build 2015;108:175–84. https://doi.org/10.1016/j.enbuild.2015.08.016.

[40] Zhou J, Zhao X, Ma X, Du Z, Fan Y, Cheng Y, et al. Clear-days operational performance of a hybrid experimental space heating system employing the novel mini-channel solar thermal & PV/T panels and a heat pump. Sol Energy 2017;155:464–77. https://doi.org/10.1016/j.solener.2017.06.056.

[41] Wang G, Zhao Y, Quan Z, Tong J. Application of a multi-function solar-heat pump system in residential buildings. Appl Therm Eng 2018;130:922–37. https://doi.org/10.1016/j.applthermaleng.2017.10.046.

[42] Fu HD, Pei G, Ji J, Long H, Zhang T, Chow TT. Experimental study of a photovoltaic solar-assisted heat-pump/heat-pipe system. Appl Therm Eng 2012;40:343–50. https://doi.org/10.1016/j.applthermaleng.2012.02.036.

[43] Zhang X, Zhao X, Shen J, Hu X, Liu X, Xu J. Design, fabrication and experimental study of a solar photovoltaic/loop-heat-pipe based heat pump system. Sol Energy 2013;97:551–68. https://doi.org/10.1016/j.solener.2013.09.022.

[44] Zhang X, Zhao X, Xu J, Yu X. Characterization of a solar photovoltaic/loop-heat-pipe heat pump water heating system. Appl Energy 2013;102:1229–45. https://doi.org/10.1016/j.apenergy.2012.06.039.

[45] Al-Sayyab AKS. Experimental Evaluation of Window-Type Air-Conditioning Unit with New Expansion Device and R404A Alternative Refrigerant. Int J Air-Conditioning Refrig 2020;28:1–9. https://doi.org/10.1142/S2010132520500315.

[46] Ali k.Shaker Al-Sayyab, Performance Enhancement of Window-Type Air-Conditioning Units, Int. J. Air-Conditioning Refrig. 26 (2018). https://doi.org/10.1142/S2010132518500128.

[47] Chen J, Yu J. Theoretical analysis on a new direct expansion solar assisted ejector-compression heat pump cycle for water heater. Sol Energy 2017;142:299–307. https://doi.org/10.1016/j.solener.2016.12.043.

[48] Xu Y, Guo F, Song M, Jiang N, Wang Q, Chen G. Exergetic and economic analyses of a novel modified solar-heat-powered ejection-compression refrigeration cycle comparing with conventional cycle. Energy Convers Manag 2018;168:107–18. https://doi.org/10.1016/j.enconman.2018.04.098.

[49] Tzivanidis C, Bellos E, Mitsopoulos G, Antonopoulos KA, Delis A. Energetic and financial evaluation of a solar assisted heat pump heating system with other usual heating systems in Athens. Appl Therm Eng 2016;106:87–97. https://doi.org/10.1016/j.applthermaleng.2016.06.004.

[50] Jie J, Jingyong C, Wenzhu H, Yan F. Experimental study on the performance of solar-assisted multi-functional heat pump based on enthalpy difference lab withsolar simulator. Renew Energy 2015;75:381–8. https://doi.org/10.1016/j.renene.2014.09.054.

[51] Bellos E, Tzivanidis C, Moschos K, Antonopoulos KA. Energetic and financial evaluation of solar assisted heat pump space heating systems. Energy Convers Manag 2016;120:306–19. https://doi.org/10.1016/j.enconman.2016.05.004.

[52] Sun X, Dai Y, Novakovic V, Wu J, Wang R. Performance Comparison of Direct Expansion Solar-assisted Heat Pump and Conventional Air Source Heat Pump for Domestic Hot Water. Energy Procedia, Elsevier Ltd 2015:394–401. https://doi.org/10.1016/j.egypro.2015.02.140.

[53] Li F, Chang Z, Li X, Tian Q. Energy and exergy analyses of a solar-driven ejector-cascade heat pump cycle. Energy 2018;165:419–31. https://doi.org/10.1016/j.energy.2018.09.173.

[54] Al-Sayyab AKS, Navarro-Esbrí J, Mota-Babiloni A. Energy, exergy, and environmental (3E) analysis of a compound ejector-heat pump with low GWP refrigerants for simultaneous data center cooling and district heating. Int J Refrig 2021;133:61–72. https://doi.org/10.1016/j.ijrefrig.2021.09.036.

[55] Xu G, Zhang X, Deng S. A simulation study on the operating performance of a solar-air source heat pump water heater. Appl Therm Eng 2006;26:1257–65. https://doi.org/10.1016/j.applthermaleng.2005.10.033.

[56] Xu Y, Jiang N, Wang Q, Mao N, Chen G, Gao Z. Refrigerant evaluation and performance comparison for a novel hybrid solar-assisted ejection-compression refrigeration cycle. Sol Energy 2018;160:344–52. https://doi.org/10.1016/j.solener.2017.12.030.

[57] Arbel A, Sokolov M. Revisiting solar-powered ejector air conditioner - The greener the better. Sol Energy 2004;77:57–66. https://doi.org/10.1016/j.solener.2004.03.009.

[58] Xu Y, Wang C, Jiang N, Song M, Wang Q, Chen G. A solar-heat-driven ejector-assisted combined compression cooling system for multistory building – Application potential and effects of floor numbers. Energy Convers Manag 2019; 195:86–98. https://doi.org/10.1016/j.enconman.2019.04.090.

[59] Wang X, Yan Y, Wright E, Hao X, Gao N. Prospect Evaluation of Low-GWP Refrigerants R1233zd(E) and R1336mzz(Z) Used in Solar-Driven Ejector-Vapor Compression Hybrid Refrigeration System. J Therm Sci 2020;29. https://doi.org/10.1007/s11630-020-1297-z.

[60] Chesi A, Ferrara G, Ferrari L, Tarani F. Analysis of a solar assisted vapour compression cooling system. Renew Energy 2013;49:48–52. https://doi.org/10.1016/j.renene.2012.01.068.

[61] Sun DW. Solar powered combined ejector-vapour compression cycle for air conditioning and refrigeration. Energy Convers Manag 1997;38:479–91. https://doi.org/10.1016/S0196-8904(96)00063-5.

[62] Dang C. Study on ejector - vapor compression hybrid air conditioning system using solar energy. Conf: Int. Refrig. Air Cond; 2012.

[63]] J. Ji, G. Pei, T. tai Chow, K. Liu, H. He, J. Lu, C. Han, Experimental study of photovoltaic solar assisted heat pump system, Sol. Energy. 82 (2008) 43–52. https://doi.org/10.1016/j.solener.2007.04.006.

[64] Kuang YH, Wang RZ. Performance of a multi-functional direct-expansion solar assisted heat pump system. Sol Energy 2006;80:795–803. https://doi.org/10.1016/j.solener.2005.06.003.

[65] J. Ji, K. Liu, T. tai Chow, G. Pei, W. He, H. He, Performance analysis of a photovoltaic heat pump, Appl. Energy. 85 (2008) 680–693. https://doi.org/10.1016/j.apenergy.2008.01.003.

[66] Xu G, Deng S, Zhang X, Yang L, Zhang Y. Simulation of a photovoltaic/thermal heat pump system having a modified collector/evaporator. Sol Energy 2009;83: 1967–76. https://doi.org/10.1016/j.solener.2009.07.008.

[67] Fang G, Hu H, Liu X. Experimental investigation on the photovoltaic-thermal solar heat pump air-conditioning system on water-heating mode. Exp Therm Fluid Sci 2010;34:736–43. https://doi.org/10.1016/j.expthermflusci.2010.01.002.

[68] Mastrullo R, Renno C. A thermoeconomic model of a photovoltaic heat pump. Appl Therm Eng 2010;30:1959–66. https://doi.org/10.1016/j.applthermaleng.2010.04.023.

[69] Zhao X, Zhang X, Riffat SB, Su Y. Theoretical study of the performance of a novel PV/e roof module for heat pump operation. Energy Convers Manag 2011;52: 603–14. https://doi.org/10.1016/j.enconman.2010.07.036.

[70] Keliang L, Jie J, Tin-tai C, Gang P, Hanfeng H, Aiguo J, et al. Performance study of a photovoltaic solar assisted heat pump with variable-frequency compressor - A case study in Tibet. Renew Energy 2009;34:2680–7. https://doi.org/10.1016/j.renene.2009.04.031.

[71] Chen H, Riffat SB, Fu Y. Experimental study on a hybrid photovoltaic/heat pump system. Appl Therm Eng 2011;31:4132–8. https://doi.org/10.1016/j.applthermaleng.2011.08.027.

[72] Wang Q, Liu YQ, Liang GF, Li JR, Sun SF, Chen GM. Development and experimental validation of a novel indirect-expansion solar-assisted multifunctional heat pump. Energy Build 2011;43:300–4. https://doi.org/10.1016/j.enbuild.2010.09.013.

[73] Ji J, He H, Chow T, Pei G, He W, Liu K. Distributed dynamic modeling and experimental study of PV evaporator in a PV/T solar-assisted heat pump. Int J Heat Mass Transf 2009;52:1365–73. https://doi.org/10.1016/j.ijheatmasstransfer.2008.08.017.

[74] Chaturvedi SK, Abdel-Salam TM, Sreedharan SS, Gorozabel FB. Two-stage direct expansion solar-assisted heat pump for high temperature applications. Appl Therm Eng 2009;29:2093–9. https://doi.org/10.1016/j.applthermaleng.2008.10.010.

[75] Cai J, Ji J, Wang Y, Huang W. Numerical simulation and experimental validation of indirect expansion solar-assisted multi-functional heat pump. Renew Energy 2016;93:280–90. https://doi.org/10.1016/j.renene.2016.02.082.

[76] Wang Y, Quan Z, Xu Z, Zhao Y, Wang Z. Heating performance of a novel solar–air complementary building energy system with an energy storage feature. Sol Energy 2022;236:75–87. https://doi.org/10.1016/j.solener.2022.02.054.

[77] Al-Sayyab AKS, Navarro-Esbrí J, Soto-Francés VM, Mota-Babiloni A. Conventional and Advanced Exergoeconomic Analysis of a Compound Ejector-Heat Pump for Simultaneous Cooling and Heating. Energies 2021;14. https://doi.org/10.3390/en14123511.

[78] Lu D, Liu Z, Bai Y, Cheng R, Gong M. Study on the multi-energy complementary absorption system applied for combined cooling and heating in cold winter and hot summer areas. Appl Energy 2022;312:118746. https://doi.org/10.1016/j.apenergy.2022.118746.

[79] Xu Y, Jiang N, Wang Q, Han X, Gao Z, Chen G. Proposal and thermodynamic analysis of an ejection–compression refrigeration cycle driven by low-grade heat. Energy Convers Manag 2017;145:343–52. https://doi.org/10.1016/j.enconman.2017.05.013.

[80] Energy Information Administration (EIA), Geothermal explained, Geothermal energy and the environment, (2022).

[81] International Renewable Energy Agency, Renewable Power Generation Costs in 2019, 2020.

[82] Lund JW. The USA geothermal country update. Geothermics 2003;32:409–18. https://doi.org/10.1016/S0375-6505(03)00053-1.

[83] The Petroleum Economist, Outlook 2023: The geothermal prize in tackling the energy trilemma, 2023.

[84] Irena, Renewable Power Generation Costs 2020, 2021. www.irena.org.

[85] A. Hepbasli, O. Akdemir, E. Hancioglu, Experimental study of a closed loop vertical ground source heat pump system, 2003. www.elsevier.com/locate/enconman.

[86] Maddah S, Goodarzi M, Safaei MR. Comparative study of the performance of air and geothermal sources of heat pumps cycle operating with various refrigerants and vapor injection. Alexandria Eng J 2020;59:4037–47. https://doi.org/10.1016/j.aej.2020.07.009.

[87] Akbulut U, Utlu Z, Kincay O. Exergy, exergoenvironmental and exergoeconomic evaluation of a heat pump-integrated wall heating system. Energy 2016;107: 502–22. https://doi.org/10.1016/j.energy.2016.04.050.

[88] EUROBSERVER, HEAT PUMPS BAROMETER, 2022. https://www.eurobserv-er.org/heat-pumps-barometer- 2020 (accessed July 17, 2022).

[89] Liu Z, Xu W, Zhai X, Qian C, Chen X. Feasibility and performance study of the hybrid ground-source heat pump system for one office building in Chinese heating dominated areas. Renew Energy 2017;101:1131–40. https://doi.org/10.1016/j.renene.2016.10.006.

[90] Cui W, Zhou S, Liu X. Optimization of design and operation parameters for hybrid ground-source heat pump assisted with cooling tower. Energy Build 2015;99: 253–62. https://doi.org/10.1016/j.enbuild.2015.04.034.

[91] Cho C, Min Choi J. Experimental investigation of a multi-function heat pump under various operating modes, Renew. Energy 2013;54:253–8. https://doi.org/10.1016/j.renene.2012.07.017.

[92] Liu X, Ni L, Lau SK, Li H. Performance analysis of a multi-functional heat pump system in cooling mode. Appl Therm Eng 2013;59:253–66. https://doi.org/10.1016/j.applthermaleng.2013.05.032.

[93] You T, Wang B, Wu W, Shi W, Li X. A new solution for underground thermal imbalance of ground-coupled heat pump systems in cold regions: Heat compensation unit with thermosyphon. Appl Therm Eng 2014;64:283–92. https://doi.org/10.1016/j.applthermaleng.2013.12.010.

[94] Qian H, Wang Y. Modeling the interactions between the performance of ground source heat pumps and soil temperature variations, Energy. Sustain Dev 2014;23: 115–21. https://doi.org/10.1016/j.esd.2014.08.004.

[95] Kim W, Choi J, Cho H. Performance analysis of hybrid solar-geothermal CO 2 heat pump system for residential heating. Renew Energy 2013;50:596–604. https://doi.org/10.1016/j.renene.2012.07.020.

[96] Yang WB, Shi MH, Dong H. Numerical simulation of the performance of a solar-earth source heat pump system. Appl Therm Eng 2006;26:2367–76. https://doi.org/10.1016/j.applthermaleng.2006.02.017.

[97] Xi C, Lin L, Hongxing Y. Long term operation of a solar assisted ground coupled heat pump system for space heating and domestic hot water. Energy Build 2011; 43:1835–44. https://doi.org/10.1016/j.enbuild.2011.03.033.

[98] Wang X, Zheng M, Zhang W, Zhang S, Yang T. Experimental study of a solar-assisted ground-coupled heat pump system with solar seasonal thermal storage in severe cold areas. Energy Build 2010;42:2104–10. https://doi.org/10.1016/j.enbuild.2010.06.022.

[99] Trillat-Berdal V, Souyri B, Fraisse G. Experimental study of a ground-coupled heat pump combined with thermal solar collectors. Energy Build 2006;38:1477–84. https://doi.org/10.1016/j.enbuild.2006.04.005.

[100] Wang E, Fung AS, Qi C, Leong WH. Performance prediction of a hybrid solar ground-source heat pump system. Energy Build 2012;47:600–11. https://doi.org/10.1016/j.enbuild.2011.12.035.

[101] Ozgener O, Hepbasli A. Performance analysis of a solar-assisted ground-source heat pump system for greenhouse heating: An experimental study. Build Environ 2005;40:1040–50. https://doi.org/10.1016/j.buildenv.2004.08.030.

[102] Ozgener O, Hepbasli A. Experimental performance analysis of a solar assisted ground-source heat pump greenhouse heating system. Energy Build 2005;37: 101–10. https://doi.org/10.1016/j.enbuild.2004.06.003.

[103] Pektezel O, Acar HI. Energy and exergy analysis of combined organic rankine cycle-single and dual evaporator vapor compression refrigeration cycle. Appl Sci 2019;9. https://doi.org/10.3390/app9235028.

[104] Bakirci K, Ozyurt O, Comakli K, Comakli O. Energy analysis of a solar-ground source heat pump system with vertical closed-loop for heating applications. Energy 2011;36:3224–32. https://doi.org/10.1016/j.energy.2011.03.011.

[105] Chen X, Yang H. Performance analysis of a proposed solar assisted ground coupled heat pump system. Appl Energy 2012;97:888–96. https://doi.org/10.1016/j.apenergy.2011.11.073.

[106] Rad FM, Fung AS, Leong WH. Feasibility of combined solar thermal and ground source heat pump systems in cold climate, Canada. Energy Build 2013;61:224–32. https://doi.org/10.1016/j.enbuild.2013.02.036.

[107] Zheng X, Li HQ, Yu M, Li G, Shang QM. Benefit analysis of air conditioning systems using multiple energy sources in public buildings. Appl Therm Eng 2016; 107:709–18. https://doi.org/10.1016/j.applthermaleng.2016.04.078.

[108] Ma H, Li C, Lu W, Zhang Z, Yu S, Du N. Experimental study of a multi-energy complementary heating system based on a solar-groundwater heat pump unit. Appl Therm Eng 2016;109:718–26. https://doi.org/10.1016/j.applthermaleng.2016.08.136.

[109] Chen Y, Wang J, Ma C, Shi G. Multicriteria performance investigations of a hybrid ground source heat pump system integrated with concentrated photovoltaic thermal solar collectors. Energy Convers Manag 2019;197:111862. https://doi.org/10.1016/j.enconman.2019.111862.

[110] Kim H, Nam Y, Bae S, Cho S. Study on the Performance of Multiple Sources and Multiple Uses Heat Pump System in Three Different Cities. Energies 2020;13: 5211. https://doi.org/10.3390/en13195211.

[111] Mukaffi ARI, Arief RS, Hendradjit W, Romadhon R. Optimization of Cooling System for Data Center Case Study: PAU ITB Data Center. Procedia Eng 2017;170: 552–7. https://doi.org/10.1016/j.proeng.2017.03.088.

[112] Davies GF, Maidment GG, Tozer RM. Using data centres for combined heating and cooling: An investigation for London. Appl Therm Eng 2016;94:296–304. https://doi.org/10.1016/j.applthermaleng.2015.09.111.
[113] He Z, Ding T, Liu Y, Li Z. Analysis of a district heating system using waste heat in a distributed cooling data center. Appl Therm Eng 2018;141:1131–40. https://doi.org/10.1016/j.applthermaleng.2018.06.036.
[114] Sheme E, Holmbacka S, Lafond S, Lučanin D, Frashëri N. Feasibility of using renewable energy to supply data centers in 60° north latitude. Sustain Comput Informatics Syst 2018;17:96–106. https://doi.org/10.1016/j.suscom.2017.10.017.
[115] Deymi-Dashtebayaz M, Namanlo SV. Potentiometric and economic analysis of using air and water-side economizers for data center cooling based on various weather conditions. Int J Refrig 2019;99:213–25. https://doi.org/10.1016/j.ijrefrig.2019.01.011.
[116] Oró E, Taddeo P, Salom J. Waste heat recovery from urban air cooled data centres to increase energy efficiency of district heating networks. Sustain Cities Soc 2019;45:522–42. https://doi.org/10.1016/j.scs.2018.12.012.
[117] Wahlroos M, Pärssinen M, Manner J, Syri S. Utilizing data center waste heat in district heating – Impacts on energy efficiency and prospects for low-temperature district heating networks. Energy 2017;140:1228–38. https://doi.org/10.1016/j.energy.2017.08.078.
[118] Oró E, Allepuz R, Martorell I, Salom J. Design and economic analysis of liquid cooled data centres for waste heat recovery: A case study for an indoor swimming pool. Sustain Cities Soc 2018;36:185–203. https://doi.org/10.1016/j.scs.2017.10.012.
[119] Al-Sayyab AKS, Navarro-Esbrí J, Barragán-Cervera A, Mota-Babiloni A. Techno-economic analysis of a PV/T waste heat–driven compound ejector-heat pump for simultaneous data centre cooling and district heating using low global warming potential refrigerants. Mitig Adapt Strateg Glob Chang 2022;27:43. https://doi.org/10.1007/s11027-022-10017-6.
[120] Deymi-Dashtebayaz M, Valipour-Namanlo S. Thermoeconomic and environmental feasibility of waste heat recovery of a data center using air source heat pump. J Clean Prod 2019;219:117–26. https://doi.org/10.1016/j.jclepro.2019.02.061.
[121] Ebrahimi K, Jones GF, Fleischer AS. Thermo-economic analysis of steady state waste heat recovery in data centers using absorption refrigeration. Appl Energy 2015;139:384–97. https://doi.org/10.1016/j.apenergy.2014.10.067.
[122] H. Chen, Y. hang Peng, Y. ling Wang, Thermodynamic analysis of hybrid cooling system integrated with waste heat reusing and peak load shifting for data center, Energy Convers. Manag. 183 (2019) 427–439. https://doi.org/10.1016/j.enconman.2018.12.117.
[123] Zhang P, Wang B, Wu W, Shi W, Li X. Heat recovery from internet data centers for space heating based on an integrated air conditioner with thermosyphon. Renew Energy 2015;80:396–406. https://doi.org/10.1016/j.renene.2015.02.032.
[124] Deymi-Dashtebayaz M, Valipour Namanlo S, Arabkoohsar A. Simultaneous use of air-side and water-side economizers with the air source heat pump in a data center for cooling and heating production. Appl Therm Eng 2019;161:114133. https://doi.org/10.1016/j.applthermaleng.2019.114133.
[125] Han Z, Zhang YY, Meng X, Liu Q, Li W, Han Y, et al. Simulation study on the operating characteristics of the heat pipe for combined evaporative cooling of computer room air-conditioning system. Energy 2016;98:15–25. https://doi.org/10.1016/j.energy.2016.01.009.
[126] Wang Z, Zhang X, Li Z, Luo M. Analysis on energy efficiency of an integrated heat pipe system in data centers. Appl Therm Eng 2015;90:937–44. https://doi.org/10.1016/j.applthermaleng.2015.07.078.
[127] Huang Q, Shao S, Zhang H, Tian C. Development and composition of a data center heat recovery system and evaluation of annual operation performance. Energy 2019;189:116200. https://doi.org/10.1016/j.energy.2019.116200.
[128] Li YM, Hung TC, Wu CJ, Su TY, Xi H, Wang CC. Experimental investigation of 3-kW organic Rankine cycle (ORC) system subject to heat source conditions: A new appraisal for assessment. Energy 2021;217:119342. https://doi.org/10.1016/j.energy.2020.119342.
[129] Quoilin S, Declaye S, Tchanche BF, Lemort V. Thermo-economic optimization of waste heat recovery Organic Rankine Cycles. Appl Therm Eng 2011;31:2885–93. https://doi.org/10.1016/j.applthermaleng.2011.05.014.
[130] Ministry of Development, Update of the Long-Term Strategy for Energy Renovation in the Building Sector in Spain, (2017) 73. https://ec.europa.eu/energy/sites/ener/files/documents/es_building_renov_2017_en.pdf.
[131] Saini P, Singh J, Sarkar J. Thermodynamic, economic and environmental analyses of a novel solar energy driven small-scale combined cooling, heating and power system. Energy Convers Manag 2020;226:113542. https://doi.org/10.1016/j.enconman.2020.113542.
[132] Liang Y, Mckeown A, Yu Z, Alshammari SFK. Experimental study on a heat driven refrigeration system based on combined organic Rankine and vapour compression cycles. Energy Convers Manag 2021;234:113953. https://doi.org/10.1016/j.enconman.2021.113953.
[133] Saleh B. Energy and exergy analysis of an integrated organic Rankine cycle-vapor compression refrigeration system. Appl Therm Eng 2018;141:697–710. https://doi.org/10.1016/j.applthermaleng.2018.06.018.
[134] Zhu Y, Li W, Wang Y, Li H, Li S. Thermodynamic analysis and parametric optimization of ejector heat pump integrated with organic Rankine cycle combined cooling, heating and power system using zeotropic mixtures. Appl Therm Eng 2021;194:117097. https://doi.org/10.1016/j.applthermaleng.2021.117097.
[135] Mounier V., Potential and Challenges of ORC driven Heat Pumps Based on Gas Bearing Supported Turbomachinery, 2018.
[136] Molés F, Navarro-Esbrí J, Peris B, Mota-Babiloni A, Kontomaris K. Thermodynamic analysis of a combined organic Rankine cycle and vapor compression cycle system activated with low temperature heat sources using low GWP fluids. Appl Therm Eng 2015;87:444–53. https://doi.org/10.1016/j.applthermaleng.2015.04.083.
[137] Saini P, Singh J, Sarkar J. Proposal and performance comparison of various solar-driven novel combined cooling, heating and power system topologies. Energy Convers Manag 2020;205:112342. https://doi.org/10.1016/j.enconman.2019.112342.
[138] Yu H, Gundersen T, Feng X. Process integration of organic Rankine cycle (ORC) and heat pump for low temperature waste heat recovery. Energy 2018;160:330–40. https://doi.org/10.1016/j.energy.2018.07.028.
[139] Liu L, Wu J, Zhong F, Gao N, Cui G. Development of a novel cogeneration system by combing organic rankine cycle and heat pump cycle for waste heat recovery. Energy 2021;217:119445. https://doi.org/10.1016/j.energy.2020.119445.
[140] Ashwni AF. Sherwani, Thermodynamic analysis of hybrid heat source driven organic Rankine cycle integrated flash tank vapor-compression refrigeration system. Int J Refrig 2021;129:267–77. https://doi.org/10.1016/j.ijrefrig.2021.05.006.
[141] Ebrahimi K, Jones GF, Fleischer AS. The viability of ultra low temperature waste heat recovery using organic Rankine cycle in dual loop data center applications. Appl Therm Eng 2017;126:393–406. https://doi.org/10.1016/j.applthermaleng.2017.07.001.
[142] A. Khalid, S. Al-Sayyab, A. Mota-Babiloni, Á. Barragán-Cervera, J. Navarro-Esbrí, Dual fluid trigeneration combined organic Rankine-compound ejector-multi evaporator vapour compression system, (n.d.). https://doi.org/10.1016/j.enconman.2022.115876.
[143] Bao J, Zhang L, Song C, Zhang N, Zhang X, He G. Comparative study of combined organic Rankine cycle and vapor compression cycle for refrigeration: Single fluid or dual fluid? Sustain Energy Technol Assessments 2020;37:100595. https://doi.org/10.1016/j.seta.2019.100595.
[144] Zheng N, Wei J, Zhao L. Analysis of a solar Rankine cycle powered refrigerator with zeotropic mixtures. Sol Energy 2018;162:57–66. https://doi.org/10.1016/j.solener.2018.01.011.
[145] Aphornratana S, Sriveerakul T. Analysis of a combined Rankine-vapour-compression refrigeration cycle. Energy Convers Manag 2010;51:2557–64. https://doi.org/10.1016/j.enconman.2010.04.016.
[146] Demierre J, Henchoz S, Favrat D. Prototype of a thermally driven heat pump based on integrated Organic Rankine Cycles (ORC). Energy 2012;41:10–7. https://doi.org/10.1016/j.energy.2011.08.049.
[147] Akrami E, Chitsaz A, Ghamari P, Mahmoudi SMS. Energy and exergy evaluation of a tri-generation system driven by the geothermal energy. J Mech Sci Technol 2017;31:401–8. https://doi.org/10.1007/s12206-016-1242-y.
[148] Javanshir N, Seyed Mahmoudi SM, Rosen MA. Thermodynamic and exergoeconomic analyses of a novel combined cycle comprised of vapor-compression refrigeration and organic rankine cycles. Sustain 2019;11:3374. https://doi.org/10.3390/su10023374.
[149] Liao G, Liu L, Zhang F, Jiaqiang E, Chen J. A novel combined cooling-heating and power (CCHP) system integrated organic Rankine cycle for waste heat recovery of bottom slag in coal-fired plants. Energy Convers Manag 2019;186:380–92. https://doi.org/10.1016/j.enconman.2019.02.072.
[150] Zhar R, Allouhi A, Ghodbane M, Jamil A, Lahrech K. Parametric analysis and multi-objective optimization of a combined Organic Rankine Cycle and Vapor Compression Cycle. Sustain Energy Technol Assessments 2021;47:101401. https://doi.org/10.1016/j.seta.2021.101401.
[151] Nasir MT, Ekwonu MC, Esfahani JA, Kim KC. Performance assessment and multi-objective optimization of an organic Rankine cycles and vapor compression cycle based combined cooling, heating, and power system. Sustain Energy Technol Assessments 2021;47:101457. https://doi.org/10.1016/j.seta.2021.101457.
[152] Li H, Bu X, Wang L, Long Z, Lian Y. Hydrocarbon working fluids for a Rankine cycle powered vapor compression refrigeration system using low-grade thermal energy. Energy Build 2013;65:167–72. https://doi.org/10.1016/j.enbuild.2013.06.012.
[153] Eisavi B, Nami H, Yari M, Ranjbar F. Solar-driven mechanical vapor compression desalination equipped with organic Rankine cycle to supply domestic distilled water and power – Thermodynamic and exergoeconomic implications. Appl Therm Eng 2021;193:116997. https://doi.org/10.1016/j.applthermaleng.2021.116997.
[154] Grauberger A, Young D, Bandhauer T. Experimental validation of an organic rankine-vapor compression cooling cycle using low GWP refrigerant R1234ze(E). Appl Energy 2022;307:118242. https://doi.org/10.1016/j.apenergy.2021.118242.
[155] Al-Sayyab AKS, Mota-Babiloni A, Navarro-Esbrí J. Performance evaluation of modified compound organic Rankine-vapour compression cycle with two cooling levels, heating, and power generation. Appl Energy 2023;334:120651. https://doi.org/10.1016/j.apenergy.2023.120651.
[156] GlobalABC/IEA/UNEP, GlobalABC Roadmap for Buildings and Construction 2020-2050, 2020.
[157] UNEP, The Kigali Amendment to the Montreal Protocol: HFC Phase-down, OzonAction Fact Sheet. (2016) 1–7. http://www.unep.fr/ozonaction/information/mmcfiles/7809-e-Factsheet_Kigali_Amendment_to_MP.pdf.
[158] Nikbakhti R, Wang X, Hussein AK, Iranmanesh A. Absorption cooling systems – Review of various techniques for energy performance enhancement. Alexandria Eng J 2020;59:707–38. https://doi.org/10.1016/j.aej.2020.01.036.

[159] Roumpedakis TC, Christou T, Monokrousou E, Braimakis K, Karellas S. Integrated ORC-Adsorption cycle: A first and second law analysis of potential configurations. Energy 2019;179:46–58. https://doi.org/10.1016/j.energy.2019.04.069.
[160] Lu F, Zhu Y, Pan M, Li C, Yin J, Huang F. Thermodynamic, economic, and environmental analysis of new combined power and space cooling system for waste heat recovery in waste-to-energy plant. Energy Convers Manag 2020;226:113511. https://doi.org/10.1016/j.enconman.2020.113511.
[161] Sun W, Yue X, Wang Y. Exergy efficiency analysis of ORC (Organic Rankine Cycle) and ORC-based combined cycles driven by low-temperature waste heat. Energy Convers Manag 2017;135:63–73. https://doi.org/10.1016/j.enconman.2016.12.042.
[162] Wang L, Roskilly AP, Wang R. Solar Powered Cascading Cogeneration Cycle with ORC and Adsorption Technology for Electricity and Refrigeration. Heat Transf Eng 2014;35:1028–34. https://doi.org/10.1080/01457632.2013.863067.
[163] Xue X-D-D, Zhang T, Zhang X-L-L, Ma L-R-R, He Y-L-L, Li M-J-J, et al. Performance evaluation and exergy analysis of a novel combined cooling, heating and power (CCHP) system based on liquid air energy storage. Energy 2021;222:119975. https://doi.org/10.1016/j.energy.2021.119975.
[164] B. Li, S. sen Wang, K. Wang, L. Song, Thermo-economic analysis of a combined cooling, heating and power system based on carbon dioxide power cycle and absorption chiller for waste heat recovery of gas turbine, Energy Convers. Manag. 224 (2020). https://doi.org/10.1016/j.enconman.2020.113372.
[165] Huang BJ, Chang JM, Wang CP, Petrenko VA. 1-D analysis of ejector performance. Int J Refrig 1999;22:354–64. https://doi.org/10.1016/S0140-7007(99)00004-3.
[166] Shestopalov KO, Huang BJ, Petrenko VO, Volovyk OS. Investigation of an experimental ejector refrigeration machine operating with refrigerant R245fa at design and off-design working conditions. Part 1. Theoretical analysis. Int J Refrig 2015;55:201–11. https://doi.org/10.1016/j.ijrefrig.2015.01.016.
[167] Boyaghchi FA, Chavoshi M. Multi-criteria optimization of a micro solar-geothermal CCHP system applying water/CuO nanofluid based on exergy, exergoeconomic and exergoenvironmental concepts. Appl Therm Eng 2017;112:660–75. https://doi.org/10.1016/j.applthermaleng.2016.10.139.
[168] Tashtoush B, Morosuk T, Chudasama J. Exergy and exergoeconomic analysis of a cogeneration hybrid solar organic rankine cycle with ejector. Entropy 2020;22. https://doi.org/10.3390/E22060702.
[169] Wang N, Zhang S, Fei Z, Zhang W, Shao L, Sardari F. Thermodynamic performance analysis a power and cooling generation system based on geothermal flash, organic Rankine cycles, and ejector refrigeration cycle; application of zeotropic mixtures. Sustain Energy Technol Assessments 2020;40:100749. https://doi.org/10.1016/j.seta.2020.100749.
[170] Boyaghchi FA, Chavoshi M, Sabeti V. Multi-generation system incorporated with PEM electrolyzer and dual ORC based on biomass gasification waste heat recovery: Exergetic, economic and environmental impact optimizations. Energy 2018;145:38–51. https://doi.org/10.1016/j.energy.2017.12.118.
[171] Du Y, Han P, Qiang X, Hao M, Long Y, Zhao P, et al. Off-design performance analysis of a combined cooling and power system driven by low-grade heat source. Energy Convers Manag 2018;159:327–41. https://doi.org/10.1016/j.enconman.2017.12.076.
[172] Ahmadi P, Dincer I, Rosen MA. Thermodynamic modeling and multi-objective evolutionary-based optimization of a new multigeneration energy system. Energy Convers Manag 2013;76:282–300. https://doi.org/10.1016/j.enconman.2013.07.049.
[173] Dai Y, Wang J, Gao L. Exergy analysis, parametric analysis and optimization for a novel combined power and ejector refrigeration cycle. Appl Therm Eng 2009;29:1983–90. https://doi.org/10.1016/j.applthermaleng.2008.09.016.
[174] Sanaye S, Refahi A. A novel configuration of ejector refrigeration cycle coupled with organic Rankine cycle for transformer and space cooling applications. Int J Refrig 2020;115:191–208. https://doi.org/10.1016/j.ijrefrig.2020.02.005.
[175] Zhao Y, Wang J, Cao L, Wang Y. Comprehensive analysis and parametric optimization of a CCP (combined cooling and power) system driven by geothermal source. Energy 2016;97:470–87. https://doi.org/10.1016/j.energy.2016.01.003.
[176] Yang X, Zheng N, Zhao L, Deng S, Li H, Yu Z. Analysis of a novel combined power and ejector-refrigeration cycle. Energy Convers Manag 2016;108:266–74. https://doi.org/10.1016/j.enconman.2015.11.019.